

THESIS

Ferhat Furkan Marol

2024



Hungarian University of Agriculture and Life Sciences

Szent István Campus, Gödöllő

Institute of Technology

Bachelor's degree

**EFFECT OF MILLING TECHNOLOGY ON SURFACE
PARAMETERS OF PA66 POLYMERS**

Insider consultant: Prof. Dr. Gábor Kalácska
University Professor

**Insider consultant's
Institute/department:** Institute of Technology

Created by: Ferhat Furkan Marol

Hungarian University of Agriculture and Life Sciences

2024

Content

1. INTRODUCTION.....	4
1.1. Task of the Thesis Work	5
LITERATURE REVIEW	6
2. POLYMERS AND FIBER REINFORCED POLYMERS	6
2.1. An Overview of Engineering Thermoplastics Reinforced with Short Glass Fibers.	6
2.2. Properties of Thermoplastics	7
3. PARAMETERS AFFECTING SURFACE QUALITY DURING MACHINING	10
3.1. Depth of Cut and Its Impact	10
3.2. The Role of Cutting Angles.....	11
3.3. Effects of Temperature Variations	13
3.4. Influence of Fiber Orientation.....	14
3.5. Effect of Spindle Speed and Feed Rate	15
4. MILLING TOOL TYPES AND THEIR EFFECTS	16
4.1. Introduction to Milling Tools	16
4.2. Types of Milling Tool	16
4.2.1. Straight-Toothed Milling Tools	17
4.2.2. Cylindrical Milling Tools	17
4.2.3. Ball-end Milling	18
4.2.4. Four-Toothed End Mills	19
4.3. Polymer Milling Tools Suggested by Producers	21
4.4. 2D Parameters of Milled Surfaces.....	21
4.4.1. Overview of the 2D Surface Parameters	21
4.4.2. Characterization of Different Milled Surfaces	22
5. CONCLUSION OF LITERATURE REVIEW	23
OWN RESEARCH WORK	23
6. PREPARATION FOR TEST	23
6.1. Materials Applied	23
6.2. Tool Applied	24
6.3. Cutting Milling and Measuring Process	24
7. RESULTS AND EVALUATION.....	30
7.1. PA66	30
7.2. PA66-GF30.....	38
8. COMPARISON OF SURFACE RESULTS	43
9. CONCLUSION	44
10. SUMMARY.....	45

1. INTRODUCTION

Polymers, with their remarkable qualities such as transparency, mechanical strength, and heat resistance, have found wide ranging applications across different industries. The demand for polymer products, especially in sectors like healthcare, automotive, (Prashanth et al., 2017) and electronics, has been steadily rising in recent years (Khairusshima et al., 2017). Milling is a commonly employed method for shaping polymers, offering versatility and efficiency in producing polymer components of different shapes and sizes. Milling polymers comes with its set of challenges due to their sensitivity to factors like melting, adhesion and vibration. These factors can cause poor quality surface finishes on polymers and plastics. Melting refers to the undesired fusion of the cutting tool and the workpiece, adhesion involves the tool sticking to the workpiece and vibration can lead to surface imperfections (Dobrocky et al., 2012). The process of milling technology is beneficial to the development of cracks and burrs in polymers, influenced by factors such as fiber orientation and temperature variations, resulting in distinct subsurface and interior differences (Izamshah et al., 2013).

Many research efforts investigated the influence of cutting parameters on the surface quality of milled polymers (Anjaneyulu et al., 2017; Ghalme et al., 2016). Other investigations have revealed that factors like feed rate, chip depth and rake angle play a substantial role in determining the surface roughness (Wu et al., 2022). Additionally, the choice of tool material and tool geometry can also significantly impact the quality of the milled surface. The manufacturing industry is in a constant state of evolution, driven by technological advancements and computer performance analysis tools stands at the forefront of this transformation. 3D Scanning Systems, in particular, are instrumental in meticulously scanning the surfaces of milled materials, facilitating the detection of defects and errors that may occur during the milling process (Logins-Torims, 2015). This technology provides invaluable data for making necessary adjustments to enhance surface quality. Algorithms programs meticulously analyze extensive datasets to predict the surface quality of milled polymers (Erzurumlu, 2005; Wu et al., 2022). These analyses serve as an excellent guide for optimizing machining parameters and selecting the appropriate tools. For example, computer performance analysis tools can fine-tune cutting speed, feed rate, and cutting depth, ensuring the achievement of the desired surface quality (Uchiyama et al., 2017). Surface defects such as burrs, pits and cracks can exert a significant influence on the quality and durability of milled materials (Khairusshima et al., 2017). These imperfections can have adverse effects on both the appearance and performance of the final product. As a result, this research seeks to understand the genesis and

alleviation of these faults in milled polymers specially Engineering polymers as PA66 30% and PA66. The primary objective of this study is to gain a deeper understanding of the formation of these imperfections, such as burrs, pits and cracks, thereby paving the way for more precise and high-quality outcomes in the domain of polymer processing. Reinforcement of engineering thermoplastics, especially materials such as polyamide 6 (PA6) and polyamide 66 (PA66), (Edwards, 1998) with short glass fiber reinforcement is used in many industries by increasing their mechanical and thermal properties. In particular, the tensile strength-cost ratio of Engineering Thermoplastics Reinforced with Short Glass Fibers exceeds carbon fibers by more than 30 times (Santrach, 1982). This reinforcement method improves the thermal performance of the material while increasing its mechanical strength and at the same time facilitating lightweight manufacturing processes. Research such as rheology (Laun, 1984) and microstructure analysis develops an in-depth understanding of the flow properties and intrinsic structure of the material, which allows for optimized results in product design and manufacturing processes. This special reinforcement technology will be more efficient and effective in the future with ongoing research and development to improve the properties of engineering thermoplastics. In this study, the main focus will be on engineering thermoplastics reinforced with short glass fibers and examining the results when milling is performed. At the micro scale, it will be focused on examining the results of isotropic fibers, with what variables and what results they will give. In tests using engineering polymers, the focus will be on finding more effective ways of use for the industry. In addition, one of the aims of this thesis is to produce precise results with a narrower range in a more specific location because the results obtained in the milling of thermoplastics have a very wide range in a very wide area. In this research, dry cutting application will be used without cooling or any lubricant.

1.1. Task of the Thesis Work

- Reveal the effect of milling technological settings on surface properties of natural and glass reinforced PA66 plates.
- Comparing the 2D surface roughness parameters (R_a , R_z , R_q , R_y) of the two selected engineering polymers.
- Examine the influence of cutting speed and feed rate on surface parameters, evaluating the materials sensitivity (change of R values) in the function of cutting speed and feed rates. To provide information on how to optimize the milling technology in terms of the required surface quality for various applications.

LITERATURE REVIEW

Within the context of milling technology, this literature review examines the field of engineering thermoplastics reinforced with short glass fibers, including isotropic fibers. This section explores the unique features and problems of these materials with an emphasis on comprehending the complexities involved in milling these polymer composites. The review examines the effects of different factors such as fiber reinforcement, processing-induced weaknesses and cutting parameters on surface quality during milling, with a focus on mechanical characteristics and industrial applications. Focusing on these areas could assist in providing terms on how to improve the milling procedure and provide better surface results when engineering thermoplastics reinforced with short glass fibers, taking into consideration both anisotropic and isotropic fiber configurations.

2. POLYMERS AND FIBER REINFORCED POLYMERS

2.1. An Overview of Engineering Thermoplastics Reinforced with Short Glass Fibers.

Extensive research aiming at improving the mechanical and thermal characteristics of engineering thermoplastics, particularly polyamide 66 glass fiber (PA66-GF30) and polyamide 66 (PA66), has shown the importance of short glass fiber reinforcing (Hessman et al., 2019). Investigations into polyolefins, polyamide 6, and polystyrene-acrylonitrile filled with glass fibers have explored a wide range of conditions, employing methodologies like simple shear flow, capillary rheometry, and uniaxial elongation. The internal structure of engineering thermoplastics is shown in Figure 1. These studies encompass a spectrum of fiber concentrations and direction ratios, drawing comparisons with unfilled and glass bead-filled melts (Laun, 1984). The importance of fiber orientation is meticulously examined.

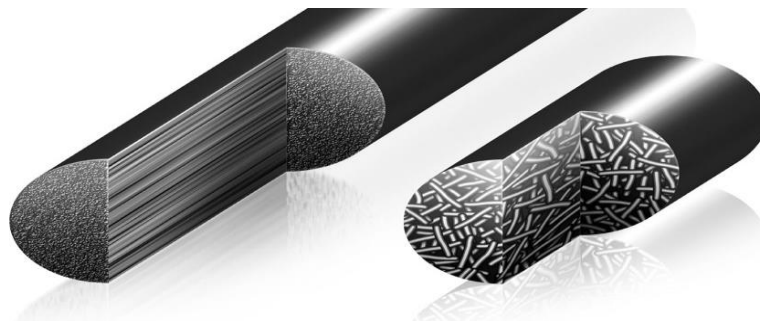


Figure 1: Internal structure of engineering thermoplastic

[<https://www.assemblymag.com/articles/94868-boosting-performance-without-breaking-the-bank>]

In recent explorations into the fatigue behavior of materials, the limitations of a binary consideration of specimen orientation in relation to the mold flow direction have become apparent (Arif et al., 2014). The binary approach, distinguishing between longitudinal and transverse orientations, lacks the depth required for accurate fatigue performance calculation (Arif et al., 2014). Addressing this limitation, earlier experiments indirectly probed the impact of orientation on fatigue behavior, establishing correlations between fatigue and strength in tensile experiments (Horst-Spoormaker, 1996). This indirect approach harnesses the progress in computational simulations, enabling the prediction of strength and stiffness in injection molded parts. Further experiments have meticulously investigated the influence of fiber concentration, length, and temperature on the shear viscosity and die swell of various short glass fiber-filled thermoplastics (Crowson-Folkes, 1980). The viscosity exhibits a substantial increase at low shear rates with both fiber length and concentration, followed by a diminishing effect at higher shear rates (Crowson-Folkes, 1980). This prompts a qualitative explanation based on insights gained from earlier fiber orientation studies. Die swell, an important parameter in mold filling, is revealed to have a strong dependence on fiber length (Crowson-Folkes, 1980). The integration of short glass fibers into thermoplastics has ushered in a new era for engineering materials, gaining significant commercial importance. While these materials offer enhanced stiffness, strength, and heat distortion temperature compared to unfilled thermoplastics, their rheological properties become intricate due to the presence of fibers. Investigating the effects of temperature, fiber length, and concentration on the viscous and elastic properties of two matrix materials, polypropylene, and nylon 6.6, has yielded valuable insights into these commercially important fiber-filled thermoplastics (Crowson-Folkes, 1980). Additionally, isotropic fiber types, which exhibit uniform properties in all directions, have gained attention for their potential applications in these thermoplastics, offering a broader scope for tailoring mechanical performance across various orientations (Lee, 1968).

2.2. Properties of Thermoplastics

Among the large number of polymers PA66 30% and PA66 are by far the most widely used polyamides worldwide. In the field of synthetic fibers, glass fibers (GF) take center stage in short fiber-reinforced polymers, offering excellent strength, stiffness, impact resistance, chemical resistance and cost-effectiveness (Edwards, 1998). The study of polymer properties spans multi-materials and demonstrates the versatility and importance of these materials in industries. One example of this research involves an in-depth investigation into the innovative integration of polyisoprene and cotton layers for the production of raincoats and tests to combine water resistance with comfort emphasizing the balance between functionality and user

satisfaction (Masuelli, 2013). The focus extends to fiber-reinforced polymer composites, where fibers embedded in epoxy or polyester resin matrices enhance strength and stiffness (Santrach, 1982). Carbon-fiber composites, exceeding steel in relative stiffness, find applications in jet aircraft components and rocket engine cases. In addition, reinforced thermoplastic resins such as polycarbonates and polyethylene are cost-effective alternatives to metals and are frequently used in household appliances and automobiles (Masuelli, 2013). In composite plastics, integrating polymers with many agents yields materials with versatile properties. Fiber-reinforced plastics focus on the intricate interplay between fiber properties, volume, length, and orientation. Mechanical properties, such as tensile, compressional, and flexural strengths, showcase the complexity of polymer design (Edwards, 1998). Examples like spandex and high-impact polystyrene illustrate the efficacy of copolymerization and blending in achieving diverse material properties.

Clear advantages, such as shape potential and efficient material utilization, are evident. Aspects related to component selection, distribution, orientation, and manufacturing processes provide a detailed perspective. Many physical properties can be understood from the core structure of PA66 (Figure 2). Discussions on short glass fibers, their commercial production, and superior tensile strength/cost performance add depth to the fiber options. Another section examines reinforced polypropylene in the automotive market (Santrach, 1982), bringing attention to its high-temperature performance, good physical properties, and cost-effectiveness. Insights into material cost savings, energy savings, and considerations related to mechanical properties affected by fiber length provide important information for designers working with fiber-reinforced plastics.

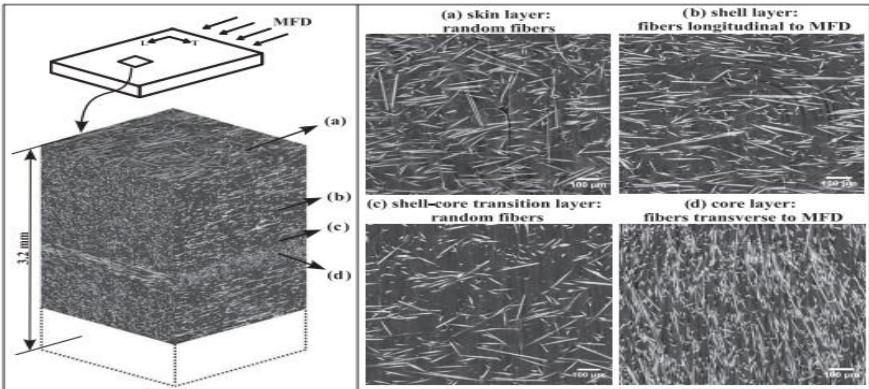


Figure 2: Skin–shell–transition–core microstructure formation of PA66 (Arif et al., 2014)

This literature review explores the issues related with processing Fiber Reinforced Plastics (FRPs), providing insight into the obstacles, range of applications, and conclusions from

previous research. Fiber Reinforced Polymers (FRPs) are composite materials made by encasing different fiber reinforcements into polymer matrices. These fibers, which are mostly composed of glass, carbon, or natural elements, are fundamental in defining the characteristics of the finished product. The material's machinability is primarily affected by processing-induced defects such as surface delamination, micro-cracks, and fiber pull-out (Pecat et al., 2012). Processing circumstances, tool choice, and processing parameters must all be carefully optimized in order to overcome these obstacles and produce the required surface quality. The primary subjects of research in the literature are the evaluation of processing parameters and the identification of factors influencing surface quality in multiple Fiber Reinforced Plastic (FRP) composite materials. Studies point out the wide range of applications for FRPs in the literature (Pecat et al., 2012; Mankar et al., 2016). A lot of industrial sectors, including sports, construction, automotive, aerospace, and others, use these materials. For example the aviation sector specifically favors Carbon Fiber Reinforced Plastics (CFRPs) due to their high strength and low weight (Khairusshima et al., 2017). To sum up, this review of the literature focuses on understanding the difficulties associated with processing fiber reinforced polymers (FRPs), improving processing methods, and facilitating the wider industrial use of these materials. These kinds of studies could lead to better materials and wider applications for FRPs. The internal structure of glass fibres is as shown in Figure 3.

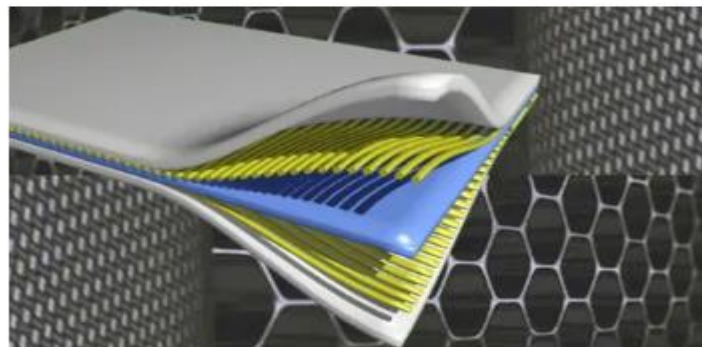


Figure 3: Glass fiber reinforced polymer

[www.alformet.com/composite/frp/gfrp]

Fiber strengthening has become an important part of polymer milling technology and it is a leading development to improve polymer surface properties. The fiber reinforcement is a major step forward in the field of material engineering in polymers matrix composites having many benefits for today's applications (Anjaneyulu et al., 2017). One of its greatest contributions is that fiber reinforcement can significantly enhance the mechanical properties of polymers. Properly applied reinforcing fibers significantly enhance overall structural integrity, flexural

strength and tensile strength. This improved mechanical performance is particularly significant in areas such as automotive design and aeronautical engineering where the strength-to-weight ratio matters (Khairusshima et al., 2017). This careful selection of fiber types allows for detailed customization of material attributes to meet specific application needs. The optimized performance that results from this personalized approach also expands the range of potential applications for polymer composites. These challenges are embodied in factors such as manufacturing complexities, cost considerations, and design intricacies.

3. PARAMETERS AFFECTING SURFACE QUALITY DURING MACHINING

3.1. Depth of Cut and Its Impact

The depth of cut is the total amount of metal removed by the tool during each pass (Figure 4). Millimeters are used to express it. It may vary depending on the type of tool and material that are employed. In mathematical terms, it is equivalent to half of the diameter difference. After reviewing earlier research, previous researches found that the depth of cut had a variety of effects on the roughness of the polymer. For instance, SPC (Stone Polymer Composite) and PVC were the materials utilized in an experiment (Wu et al., 2022). One of the most important factors in influencing the observed results was the depth of milling, which varied from 0.5 to 2 mm. As the milling depth increased, the SDR (surface damage roughness) increased from 6.8% to 28.0% (Wu et al., 2022). The pits, irregular sized depressions, on the damaged surface were found to be remarkable. These were attributed to the forces applied by the cutter during milling exceeding the adhesion strength between the CaCO₃ particles and the PVC. Larger CaCO₃ particles broke away from the surrounding PVC, resulting in the formation of pits, which were particularly evident at a milling depth of 0.5 mm (Wu et al., 2022).

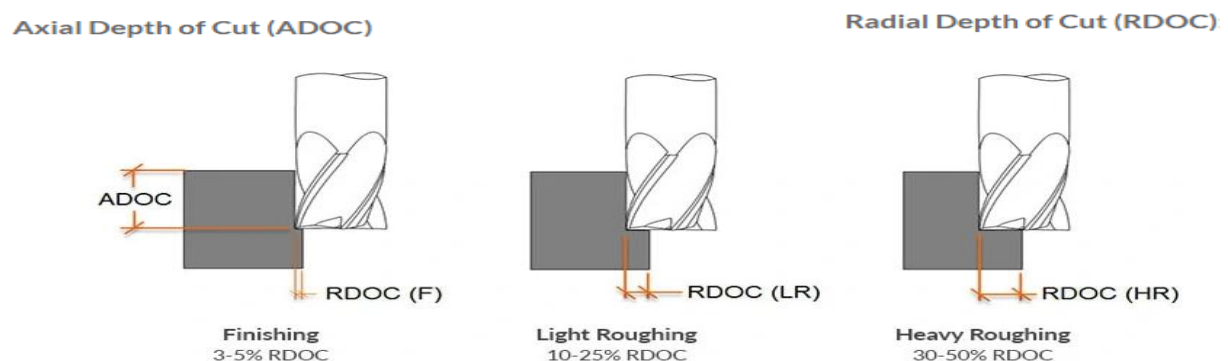


Figure 4: Depth of cut visual expression

[<https://www.harveyperformance.com/in-the-loupe/depth-of-cut/>]

The milling of Stone Polymer Composite (SPC), primarily composed of PVC and CaCO₃, has brought to light the occurrence of cracks. The CaCO₃ particles, characterized by their hardness but limited toughness, undergo cutting, compression to generate planes parallel to the material surface, or fracture under the pressure exerted by the cutter (Wu et al., 2022). These effects become more pronounced with variations in milling depth. The consistent milling waves observed on machined SPC surfaces, attributed to the cycloidal movement of the cutter during peripheral up-milling, manifest as curved tracks on the surface (Wu et al., 2022). Researchers have discerned a connection between milling depth and the Surface Damage Rate (SDR). Greater milling depths correspond to an elevated SDR, indicating an escalation in surface damage. This revelation is important for comprehending the implications of different milling depths on surface integrity, as deeper milling depths result in a higher SDR. In a separate study (Wang et al., 2021) involving curved CFRP (curved carbon fiber-reinforced plastic) composites, an investigation aimed to determine the optimal depth of cut for surface roughness. The axial cutting depth surfaced as an important factor influencing both the appearance and damage of the machined surface. Suggested parameters to minimize corrugated surface formation and machining damage included a 0.5 mm axial cutting depth. Considering machining deformation, the theoretical values for residual height exhibited a trend on the corrugated surface similar to the experimental values (Wang et al., 2021). Analyzing residual height at various axial cutting depths disclosed a gradual increase in values with higher cutting depths. This phenomenon was associated with a larger volume of removed carbon fibers and the resin matrix, leading to softening and adherence to the processed surface, resulting in suboptimal surface quality (Wang et al., 2021). The lower edge of the tool was noted to compress and slide on the machined surface during milling, inducing plastic deformation and a scratching effect, intensifying the rise in residual height (Wang et al., 2021). It was suggested that, within a specific range of milling parameters, selecting a smaller cutting depth could prove advantageous in mitigating the cumulative negative effects on residual height (Wang et al., 2021).

3.2. The Role of Cutting Angles

The quality of the machining process is directly impacted by the cutting angle, which is the angle of the cutting edge with respect to the workpiece's surface. To get the best results in micro-milling, one must investigate the ideas of cutting angles, particularly the side edge angle and tool angle (Saptaji et al., 2012). For milling, the side edge and overall angle of the milling tool must be strengthened. In order to strengthen the edge, the side edge angle entails angling the edge beyond the standard 90 degrees (Saptaji et al., 2012). 45,35 and 25 degree helix angle

cutting tool is shown in Figure 5. Concurrently, the milling tool's overall angle has a major effect on the process's outcome by affecting how it interacts with the workpiece and the deformations that arise from that interaction.



Figure 5: Solid carbide end mill with different helix angles (Anjaneyulu et al., 2017)

In this context, comprehensive experimental studies have been conducted to understand the effects of side edge angle and tool angle in micro-milling of aluminum alloys (Saptaji et al., 2012). Using aluminum alloy Al6061-T6, experiments were designed to vary the side edge angle and tool angle in different configurations. The resulting top burrs were qualitatively and quantitatively examined using scanning electron microscopy and a surface profiler. The results indicate that reinforcing the side edge and elevating the tool angle effectively diminish top burrs in micro-milling. These adjustments result in a more resilient side edge, reducing plastic deformation on the workpiece and minimizing the occurrence of top burrs. Moreover, an increased tool angle yields a similar outcome in curbing top burrs (Saptaji et al., 2012). The cutting angle edge outer surface cutting diagram is as shown in Figure 6.

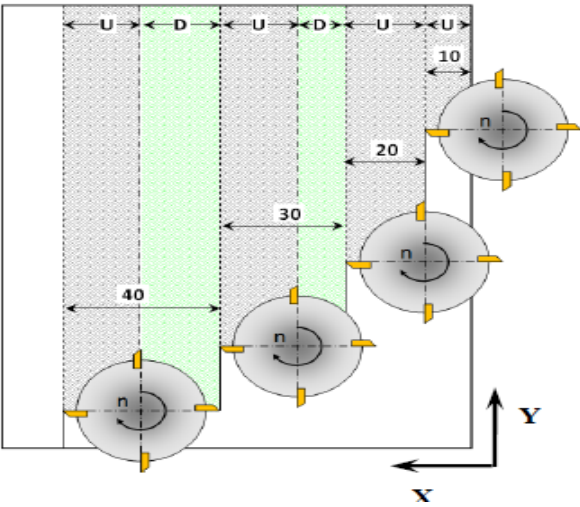


Figure 6: Cutting angle edge outer surface cutting diagram (Sorrentino-Turchetta, 2011)

3.3. Effects of Temperature Variations

In the case of polymer milling, temperature is serious consideration that cannot be ignored, exerting a significant influence on the integrity of the machined surface. In the investigation of temperature types during milling, micrographs of specimens machined at different temperatures (Figure 7), it was observed that lower temperatures, such as -40°C and 20°C , induced the formation of characteristic cracks along the machined surface (Pecat et al., 2012). These cracks, with an inclination of approximately 18° to the surface and lengths of up to $200\ \mu\text{m}$, indicated an increased fragility of the matrix material at lower temperatures (Pecat et al., 2012). As the workpiece temperature increased to 80°C , the surface became relatively smooth, and the prevalence of cracks diminished. However, at an elevated temperature of 120°C , an altered sub-surface structure was evident, suggesting potential thermal damage (Pecat et al., 2012).

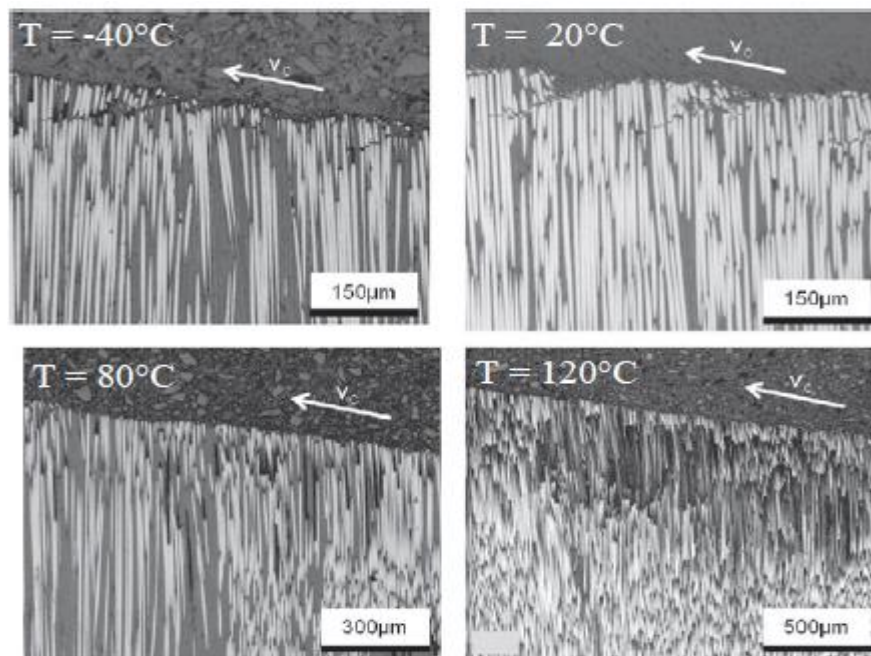


Figure 7: Micrographs of specimens machined at different temperatures (Pecat et al., 2012)

The cutting forces exhibited a noticeable regressive trend with an increase in workpiece temperature. The highest cutting force of $310\ \text{N}$ was recorded at a cutting speed of $20\ \text{m/min}$ and a workpiece temperature of -40°C , while a decrease in cutting force was observed with rising temperature (Pecat et al., 2012). This finding suggests that there an optimal operational temperature range exists, as extremely low temperatures can lead to high cutting forces, and excessively high temperatures may result in thermal damage. Machining also includes the processing of technical plastics (polymers) utilizing standard metalworking and woodworking machines. However, because to the inherent low thermal conductivity and melting point of technical plastics, strict temperature control throughout the machining process is required,

along with effective heat dissipation from the workpiece. This heat load has a major influence on both the machining dynamics and the resulting surface quality and component deformation. Coolants, which are common in metalworking, and compressed air are routinely used to alleviate excessive heat (Dobrocky et al., 2012). The temperature at the point of contact between the component's surface and the tool, as well as the use of coolants, the status of the cutting tool, and machining conditions (e.g. speed, cutting speed, feed, depth of cut), all have an impact on the quality of the machined surface of technical plastics. This emphasizes the vital need of maintaining the correct temperature during plastic component machining. Aside from the cooling medium and the careful tool selection, the delineation of optimal cutting conditions emerges as an important element in controlling the machining temperature.

3.4. Influence of Fiber Orientation

Fiber orientation has an important role in influencing the polymer milling process, significantly impacting both surface quality and damage mechanisms. A comprehensive understanding of the effects of fiber orientation is indispensable for optimizing cutting parameters and attaining the desired surface outcomes. The impact of fiber orientation on milling processes unveils distinct outcomes. In specimens with a fiber orientation of 90° , the frequent observation of cracks extending from the milled surface at an angle of 18° , with lengths of approximately 200 microns, indicates the brittle material response of CFRP (Pecat et al., 2012). This phenomenon suggests that fibers beneath the surface are breaking, inducing cracks parallel to the surface.

On the contrary, smoother surfaces with minimal damage were achieved with 0° and $+45^\circ$ fiber orientations (Figure 8). Fiber bending near the machined surface, particularly at higher cutting speeds, was observed. Cutting forces exhibited significant variations based on fiber orientation, with the most substantial difference observed between $+45^\circ$ (300 N) and -45° (60 N) (Pecat et al., 2012). This emphasizes how important fiber orientation is for establishing cutting forces and maintaining surface integrity while milling polymers. Striking a balance between the advantages and disadvantages of different orientations emerges as a significant issue for optimizing milling processes.

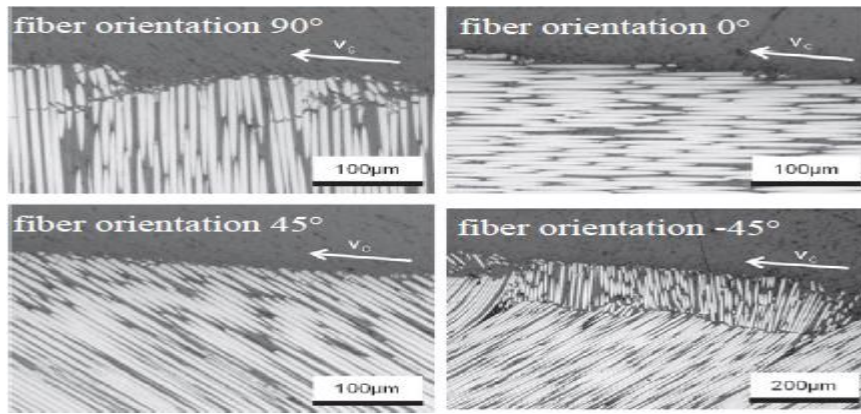


Figure 8: Micrographs of specimens with different fiber orientations (Pecat et al., 2012)

3.5. Effect of Spindle Speed and Feed Rate

Spindle speed, signifying the rotational velocity of the cutting tool around the workpiece, directly governs the machining velocity. Conversely, feed rate dictates the traversal speed of the cutting tool across the workpiece. These two parameters, spindle speed and feed rate, are paramount in configuring surface quality, mitigating damage, and optimizing efficiency throughout milling operations.

The tool feed and axial cutting depth have major effects on the damage and quality of the machined surface. To diminish corrugation and damage, a recommended setting involves an axial cutting depth of 0.5 mm and a tool feed speed of 300 mm/min. Envision a shift in the feed speed from 300 mm/min to 1000 mm/min – such alterations typically yield increased material removal rates, potentially influencing surface finish and tool wear. Higher spindle speeds, like 5000 mm/min, predominantly curtail machining damage with nominal impact on corrugated surface aesthetic (Wang et al., 2021). Imagine specimens processed at a cutting speed of 100 m/min – a transition to higher speeds, say 500 m/min –, may result in alterations in surface integrity.

Characteristic cracks may diminish or vanish, yet the risk of thermal damage could escalate. Optimal surface integrity for CFRP materialized with a fiber orientation of 0° or +45°, a workpiece temperature of 80°C, and a high cutting speed (Rentsch et al., 2012). In conclusion, surface roughness proves indispensable for medical implants such as cervical disc implants, aiming to mitigate friction and wear at the micro and nanoscale (Izamshah et al., 2013). Machining parameters significantly wield influence on surface roughness, with feed rate at the forefront, trailed by milling speed and depth of cut. High-Speed Milling (HSM) significantly enhanced die molds, focusing on precision, efficiency, and surface quality. The implementation of HSM minimized surface irregularities and ensured finer finishes compared to traditional

methods. Because it completes tasks more quickly and yields a more inexpensive outcome. It demonstrated increased material removal rates, enhancing manufacturing efficiency while maintaining optimal surface integrity. HSM's versatility was evident in effective machining of various materials, including alloy steels used in die/mold production. Conclusive results highlighted its seriousness functions that material qualities and machining approach play in maximizing outcomes (Logins-Torims, 2015).

High-Speed Milling (HSM) applied to machine technical plastics, specifically POM-C and PA 6, yielded positive results. Variations in turning speed had minimal impact on surface roughness parameters for Ertacetal C, indicating stability under different speeds. The study determined optimal cutting parameters, important for minimizing delamination and surface roughness in milled composites (Dobrocky et al., 2021). Feed rate and cutting speed demonstrated substantial influence on delamination and surface roughness, with lower feed rates and higher cutting speeds yielding superior outcomes. Multiple linear regression models provided a predictive tool for correlating cutting parameters with delamination and surface roughness (Dobrocky et al., 2021).

4. MILLING TOOL TYPES AND THEIR EFFECTS

4.1. Introduction to Milling Tools

Milling tools, which help greatly to the precision and efficiency of material removal in manufacturing. Tools are many kinds of cutting equipment used to shape and mold workpieces during the milling process. The efficiency of milling processes is heavily depended on the right selection and application of these instruments. End mills, face mills, and ball mills, for example, each serve a specific purpose in achieving desired machining results.

Milling tools are intensively researched for their uses in many types of industries, including aerospace, automotive, and general manufacturing. Optimizing machining techniques and obtaining superior surface finishes requires a thorough understanding of the features and functions of different milling equipment. The literature investigates factors impacting milling tool performance such as material composition, coatings.

4.2. Types of Milling Tool

The selection of milling tools is an important consideration in the area of machining, directly influencing the accuracy and efficiency of material removal processes. This section aims to provide an in-depth examination of multiple milling tools, emphasizing their distinct properties, applications, and significant impact on polymer surface parameters.

4.2.1. Straight-Toothed Milling Tools

Straight-toothed milling cutters with polycrystalline diamond (PCD) characteristics, in particular, are frequently used in chip removal procedures in polymer machining (Figure 9). One study shows (Wu et al., 2022) that Micrographs of milled surfaces show distinct patterns that are impacted by variables such as rake angles, spindle speed, cutter feed, and milling depth.

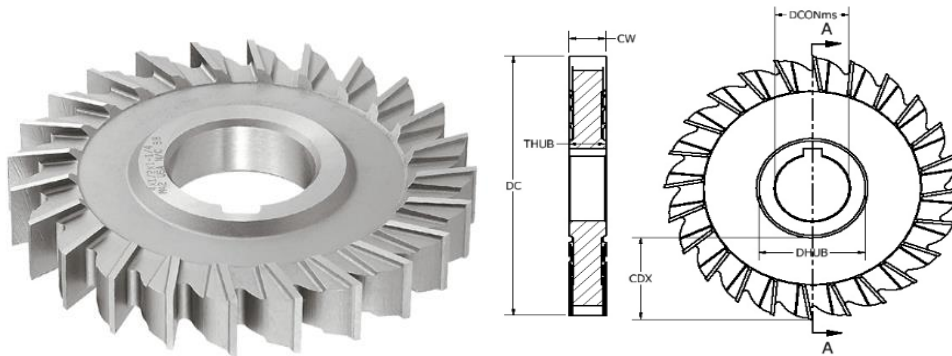


Figure 9: Standard Type Straight-Tooth Cutter

[<https://www.archcuttingtools.com/product/05000/>]

Surface modifications are indicated by the appearance of regular milling waves during straight-toothed milling, with damages mostly focused on peaks and in the axial direction, manifesting as pits and fissures. The study shows surface damage rates (SDR) and surface roughness (Ra) as critical standards for evaluating milling quality. It definitively demonstrates an inverse link between SDR and Ra with rake angle and spindle speed, while seeing a positive association with feed rate and milling depth.

This deep knowledge forms the basis for improving straight-toothed milling settings with the explicit purpose of lowering Ra values. The use of PCD straight-toothed milling cutters with six teeth and a constant diameter of 140 mm improves the reliability and effectiveness of the milling process in polymer machining even more (Wu et al., 2022).

4.2.2. Cylindrical Milling Tools

The effectiveness of milling technology on polymer surface parameters is significantly affected by cylinder milling tools, such as the Cylindrical Finishing Milling Cutter, Cylindrical Roughing Milling Cutter, Cylindrical Roughing Milling Cutter (Multiple Connected Flutes), and Cylindrical Powerful Roughing Milling Cutter (Semi-Circular Flute) (Figure 10). The carbide flutes on these tools increase stiffness during side milling operations on large workpieces. With its many linked flutes, the Cylindrical Roughing Milling Cutter reduces breakage during heavy milling and guarantees rapid and effective rough machining.

Additionally, in comparison to conventional roughing end mills, the Cylindrical Powerful Roughing Milling Cutter exhibits better milling speed and cutting capacity thanks to its semi-circular flute design. Wang (2021) emphasizes the significance of these cylindrical milling cutters in achieving optimal material removal in the surface milling process. The study explores the complex deformations observed in carbon fiber-reinforced plastics (CFRP) during curved surface milling, proposing a novel residual height calculation method to quantify material removal quality. The research, conducted on CFRP semi-cylindrical components, explores the influences of process parameters on surface appearance and machining damage, offering valuable insights for improving milling quality in polymer machining (Wang et al., 2021). Additionally, Dobrocky (2021) conducted milling experiments using a cylindrical face milling cutter on a CNC machine, emphasizing the production of brittle chips and burrs during the milling process on technical plastics. These findings accentuate the need for a comprehensive understanding of tool selection and milling parameters for efficient polymer surface milling (Dobrocky et al., 2021).



Figure 10: Cylindrical Milling Cutters

[<https://en.yeongyih.com.tw/cylindrical-milling-cutter.htm>]

4.2.3. Ball-end Milling

The ball-end milling process, when applied to polymer components using rounded-end milling cutters as shown Figure 11, has shown significant implications for surface quality and material removal efficiency. In the study conducted by Wang et al. (2021), a diamond-coated carbide ball-end mill with a diameter of 10 mm and four teeth played a pivotal role in achieving precision during the milling process. The emphasis was on curved CFRP surfaces that were

produced by rounded-end milling. This exposed the regular corrugated surface development and addressed the mechanical damages that ensued as well as their effects on surface quality (Wang et al., 2021).

The production of regular corrugated surfaces was evident in the appearance features of the curved CFRP surface components that were created by ball-end milling (Wang et al., 2021). This phenomenon was attributed to the overall deformation of the workpieces in the out-of-plane direction during the machining process, cutting through different directions of fiber layers (Wang et al., 2021). When the fiber was not properly restrained, mechanical damages were seen at the edges of the corrugated surface, which degraded the component's sealing ability and surface quality. The study focused on the creation of corrugated surfaces, the distribution of machining damage, and important variables influencing machining surface appearance (Wang et al., 2021). It offered insightful information on the subtle effects of ball-end milling on polymer surface properties. These results advance our knowledge of how polymer component surface properties are impacted by the ball-end milling process (Wang et al., 2021).



Figure 11: Tool morphologies of the ball-end mill bits (Wang et al., 2021)

4.2.4. Four-Toothed End Mills

With the unusual four-toothed and four-fluted design as shown Figure 12, four-toothed end mills effectively shape polymer blocks (Shukor et al., 2016). These tools are highly successful

rapidly shaping raw polymer blocks into desired shapes. However, the results of the research emphasize that the effectiveness of this procedure depends on skillfully controlling cutting forces to prevent negative surface heating (Shukor et al., 2016). The particular choice of cutting tools, aluminum 7075-T6, with four teeth and a diameter of 10 mm, that are utilized to mill testing surfaces inside the mold cavity is a calculated decision that is impacted by mechanical and chemical properties (Sorrentino-Turchetta, 2011; Oktem et al., 2005). The overall quality of machined surfaces is greatly enhanced by this meticulous tool selection, which also affects milling efficiency. In order to create a solid database for future machinist references, the literature in the field recommends a thorough approach that includes multiple types of machining operations, cutting tools, new materials, high spindle speeds, and varied machining processes (Shukor et al., 2016). Further emphasizing the complex relationship between surface roughness, different process parameters, and cutting force components are insights obtained from experiments conducted with carbide end mills (Sorrentino-Turchetta, 2011). The intricate considerations of variables like tool geometry and feed speed stress the importance of a methodical approach to maximize outcomes. This body of knowledge emphasizes how important it is to carefully evaluate the cutting parameters in polymer milling processes in order to simultaneously improve both efficiency and surface quality (Bayraktar-Turgut, 2016). In summary, careful consideration of cutting parameters is essential for enhancing both efficiency and surface quality in polymer milling processes, especially when utilizing four-toothed end mills.

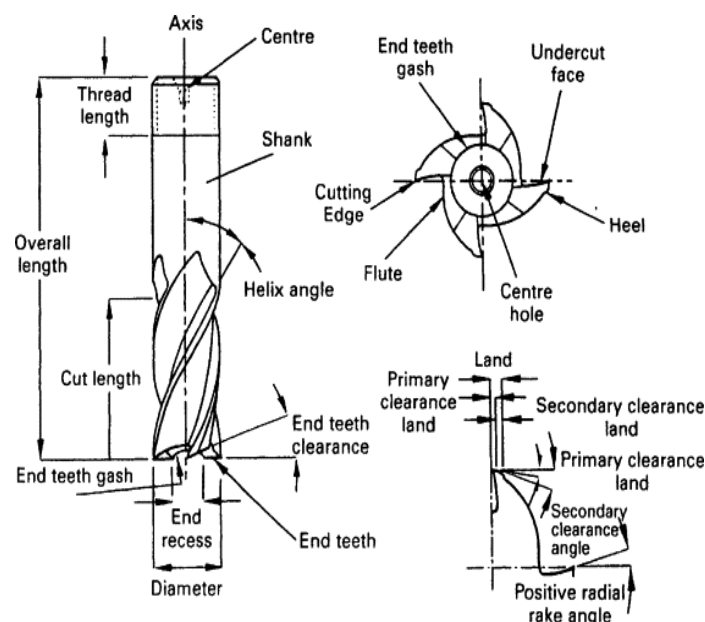


Figure 12: End mill cutter geometry (Chiles et al., 1996)

[<https://www.sciencedirect.com/topics/engineering/end-mill>]

4.3. Polymer Milling Tools Suggested by Producers

One of the tools that are suggested for use in polymer applications are single-flute end mills. These tools have a single cutting edge that is appropriate for softer materials, allowing for effective chip evacuation and reducing heat production while performing different types of machining. End mills coated with diamonds provide longer wear resistance and increased durability during extended milling operations. Because they are good at 3D profiling and sculpting and can create smooth contours on polymer surfaces, carbide ball-end mills are preferred. Especially in plunge and pocket milling, upcut spiral router bits, made for CNC machining, improve surface finishes and make chip evacuation easier. Polycrystalline Diamond (PCD) end mills are ideal for high-precision work in complex polymer components because of their remarkable wear resistance and hardness, which are attributed to their diamond-tipped cutting edges. Manufacturers can optimize their polymer milling processes by considering the specific properties of the material and consulting tooling suppliers for tailored recommendations.

4.4. 2D Parameters of Milled Surfaces

In this chapter, I aim to present a review of 2D surface parameters, focusing our attention on important indicators such as arithmetic mean roughness (R_a), maximum height/peak (R_y) and ten-point mean roughness (R_z). These measurements are indispensable benchmarks for characterizing milled surfaces in industrial contexts. The definitions and results of each parameter are meticulously outlined, providing a basic understanding of their importance in the assessment of surface quality (Kalácska, 2020).

4.4.1. Overview of the 2D Surface Parameters

Exploring 2D surface parameters involves a focused examination of micro-geometrical features for understanding machined surfaces. Arithmetical Mean Roughness (R_a) is a key parameter, determined by sampling a standard length from the mean line on the roughness chart using a Cartesian coordinate system (Figure 13). Expressed in micrometers (μm), R_a serves as a baseline for evaluating subsequent milling processes, aligning with the x-axis and magnifying along the y-axis (Kalácska, 2020). Moving deeper into the parameters, Maximum Height/Peak (R_y) gains significance by analyzing a standard length section from the mean line on the roughness chart. R_y measures the distance between peaks and valleys along the y-axis, providing insights into surface irregularities. Expressed in micrometers (μm), R_y helps comprehend overarching topographical variations influencing milled surface functionality. As a sectional analysis unfolds along the y-axis, R_z captures surface irregularities by averaging the five tallest peaks

(Y_p) and the five lowest valleys (Y_v) (Kalácska, 2020). This culmination, expressed in micrometers (μm), offers a panoramic perspective on surface characteristics, enriching our understanding by considering both peaks and valleys (Kalácska, 2020).

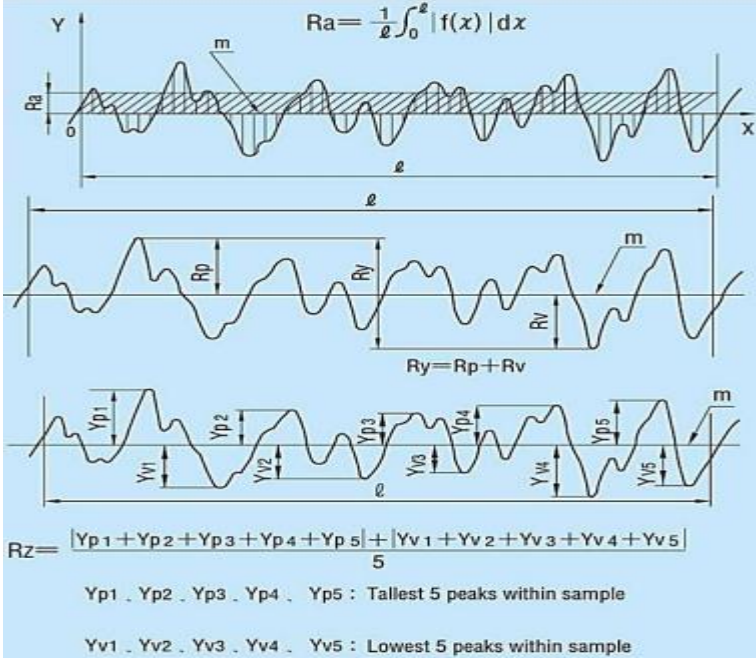


Figure 13: Variety of surface roughness indicators and typical calculations (JISB0031. (1994) Technical Data Surface Roughness)

4.4.2. Characterization of Different Milled Surfaces

Characterizing the milled surfaces is the first step towards understanding how milling method influences surface attributes of polymer components, such as surface finish, dimensional accuracy, and mechanical qualities. Tailored techniques are critical, as indicated by recommendations such as using high-speed steel (HSS) tooling for most thermoplastics and carbide tooling for reinforced materials (Curbell Plastic, 2023). Surface quality is significantly impacted by a number of variables, including clamping pressure, feed rate, and spindle speed. The use of appropriate clamping procedures can prevent material distortion; feed rates up to 0.55 mm/tooth are recommended (Curbell Plastic, 2023). By producing accurate thread profiles, threading and tapping processes aid in the characterisation of milled surfaces. Specifically, plastic materials notch sensitivity means that threading and tapping operations require extreme precision (Mitsubishi Chemical Group, 2023). To lower the chance of tearing and guarantee thread precision, coolants and single-point threading with carbide inserts are advised (Mitsubishi Chemical Group, 2023). The need of precision is emphasized by certain requirements, like the need for four to five 0.001" passes at the end (Mitsubishi Chemical Group, 2023). Managing vibrations, controlling heat generation, and

making sure the right support structures are in place are all necessary to achieve the ideal surface parameters (Boedeker Plastics, 2023). To avoid problems like cracks, crazing, or melted surfaces, for example, drills must be sharp during drilling operations; specific recommendations should be given based on the diameter and material of the hole (Boedeker Plastics, 2023). The characterization of different milled surfaces is integral to understanding the effects of milling technology on polymer component surface parameters.

5. CONCLUSION OF LITERATURE REVIEW

The main goals of the thesis work are emphasized in the literature review's conclusion. These goals are to clarify the complex interactions between surface roughness parameters and cutting technology factors that are unique to glass fiber-reinforced polyamide 6 and polyamide 66. Although the articles under review have clearly contributed to our knowledge of the general rules governing polymer machining and the range of effects of different cutting tools and parameters, there is a clear lack of information in the literature regarding the subtle effects of particular cutting parameters on surface roughness in the context of polyamides reinforced with glass fiber. Even with the abundance of research in this area, there is noticeably still no thorough synthesis outlining the precise impact of variables like cutting speed, feed rate, and depth of cut on surface quality.

Therefore, the main goals of this research project include providing an in-depth analysis of the complex relationship between cutting parameters and surface roughness and promoting additional studies to improve and optimize machining techniques specifically designed for glass fiber-reinforced polyamides. Through the investigation of this important knowledge gap and the provision of practical guidance on how to optimize the machining processes for these materials, this thesis aims to significantly advance manufacturing techniques and improve product quality in pertinent industrial domains. By showing the necessity of targeted research in this field, this study seeks to highlight the significance of ongoing investigation and improvement in the quest for excellence in polymer machining techniques.

OWN RESEARCH WORK

6. PREPARATION FOR TEST

6.1. Materials Applied

The materials used in the tests were PA66 and PA66-GF30. PA66, also known as polyamide or nylon 6.6, is a thermoplastic polymer known for its high strength, hardness, and thermal

resistance. It is also recognized for its chemical resistance and electrical insulation properties. On the other hand, PA66-GF30 is a composite material where PA66 polymer is reinforced with glass fibers. This addition enhances the material's mechanical properties, providing increased temperature tolerance and strength. Both materials find extensive industrial use, particularly in the automotive and engineering sectors.

6.2. Tool Applied

Initially, the preparation involved cutting PA66 and PA66-GF30 polymers using the PILOUS TMJ model manual cutting machine and water-based emulsion for lubrication. For milling, the MAS brand milling machine, known for its capacity to achieve a feed rate of 790 mm/min and a spindle speed of 1000 m/s, was utilized. Clamps were used to securely fix the polymers in the machining center. The milling tool, ID number F3042.B.063.Z06.15, manufactured by WALTER, was employed with specifications including a cutting diameter of 63 mm, maximum cutting depth of 15 mm, and maximum rotational speed of 12600 1/min. Surface measurements were conducted using the MITUTOYO 178-039 SURFTEST SJ-400 series, with a 10" x 16" x 2.3" granite base providing stability and precise positioning. The setup ensured accurate and consistent measurements with a maximum traversing range of 200 mm in the column Z-axis and a granite plate flatness of 8 μ m.

6.3. Cutting Milling and Measuring Process

Initially, our preparation began with cutting PA66 and PA66 Glass Fiber 30% (PA66-GF30) reinforced polymers. The PILOUS TMJ model manual cutting machine was employed for this purpose as shown in Figure 14, with the additional support of water-based emulsion during cutting. Additionally, no calculations will be made regarding the cut surfaces; they are solely relevant for the division of the pieces.



Figure 14: Photograph of cutting machine

Each polymer block was divided into 9 equal parts using this machine as shown in Figure 15. In terms of color, there were 9 pieces of white-colored PA66 and 9 pieces of black-colored PA66-GF30. Consequently, a total of 18 polymer test specimens were obtained.



Figure 15: Photograph of the polymers after the cutting process

After completing the cutting process, I transitioned to the crucial milling cutting stage. Here, I made determinations for the required spindle speed and feed rate for each piece. Following the determination, I prepared a list for the feed rate and spindle speed.

Table 1: The Table of Spindle Speed and Feed Rate Values for Testing

Depth of cut=1.5mm	PA 66	PA 66-GF30
Spindle speed n1 (rpm) 200, Max circumferential speed 0,66 m/s	Table feed rate 1 (mm/min) 100 1.	Table feed rate 1 (mm/min) 100 1.
	Table feed rate 2 (mm/min) 290 2.	Table feed rate 2 (mm/min) 290 2.
	Table feed rate 3 (mm/min) 790 3.	Table feed rate 3 (mm/min) 790 3.
Spindle speed n2 (rpm) 500 Max circumferential speed 1,65 m/s	Table feed rate 1 (mm/min) 100 4.	Table feed rate 1 (mm/min) 100 4.
	Table feed rate 2 (mm/min) 290 5.	Table feed rate 2 (mm/min) 290 5.
	Table feed rate 3 (mm/min) 790 6.	Table feed rate 3 (mm/min) 790 6.
Spindle speed n3 (rpm) 1000 Max circumferential speed 3,3 m/s	Table feed rate 1 (mm/min) 100 7.	Table feed rate 1 (mm/min) 100 7.
	Table feed rate 2 (mm/min) 290 8.	Table feed rate 2 (mm/min) 290 8.
	Table feed rate 3 (mm/min) 790 9.	Table feed rate 3 (mm/min) 790 9.
Total diameter 63 mm		

As shown in Table 1, 9 test setups were created for both PA66 and PA66-GF30. Spindle speed was divided into 3 categories: 200 n1, 500 n2, and 1000 n3. Each category was tested with 3 different feed rates. For example, when the spindle speed was set to 200 n1, part 1 was tested with a feed rate of 100 (mm/min), part 2 with a feed rate of 290 (mm/min), and part 3 with a feed rate of 790 (mm/min), and the same procedure was applied to all categories. The objective was to observe changes in surface roughness with 3 different spindle speeds, each tested with 3 different feed rates. In this process, the depth of cut was kept constant at 1.5 mm for both polymers. After determining the appropriate speed and feed parameters for our tests, I have opted to utilize the MAS brand milling machine, identified by the serial number 7196. The rationale behind selecting this particular machine from its capacity to attain a feed rate of 790 (mm/min) and a spindle speed of 1000 (m/s). Moreover, this machine offers versatility in movement along the x/y/z axes. Our decision to employ this specific equipment for the milling operation of black-colored PA66-GF30, as shown in Figure 16, is rooted in its technical capabilities aligning with the requirements of our experimentation.



Figure 16: Photograph of the polymers during the milling process

As shown in Figure 17, I utilized a machine element for the fixation of polymers in the machining center by employing clamps. This machine element ensures that polymers remain securely fixed in the machining center, ready for milling, by applying consistent pressure each time without exerting excessive force.



Figure 17: Fixation of polymers by using clamps in the machining centre

The milling tool to be used for the operation, with the ID number F3042.B.063.Z06.15, is manufactured by WALTER. It is depicted in Figure 18. Its overall length is 40 mm. The cutting diameter measures 63 mm. This tool features a maximum cutting depth of 15 mm and is capable of operating at a maximum rotational speed of 12600 1/min. Additionally, it is designed with a tool cutting edge angle of 90 degrees and possesses six peripheral effective cutting edges as well as six face effective cutting edges. The body material of the tool is solid steel. Furthermore, the parameter specifications of the tool are illustrated in Table 2.



Figure 18: Photographs of the milling tool

Table 2: Tool parameters

Material	Parameters
Face effective cutting edge count	6
Cutting diameter	63 mm
Tool cutting edge angle	90 degree
Ramping angle maximum	2.6 degree
Maximum rotational speed	12600 1/min
Overall length	40 mm
Maximum cutting depth	15 mm

In the next phase, which is the measurement stage, my goal is to see how the milling process affected each polymer component's surface roughness. I took measurements on the milled surfaces of all the components, including 30 mm sections. Each test piece underwent three repeated measurements using the MITUTOYO 178-039 SURFTEST SJ-400 series. This instrument stand is designed specifically for use with Mitutoyo's SJ-400 series of surface roughness testers. Moreover, our surface roughness analysis setup includes a 10" x 16" x 2.3" granite base, which provides stability, along with a 9.8" vertical adjustment range for precise positioning. With a maximum traversing range of 200 mm in the column Z-axis and a granite plate flatness of 8 μm , our setup ensures accurate and consistent measurements. Weighing 20 kg, it remains stable throughout the analysis process.

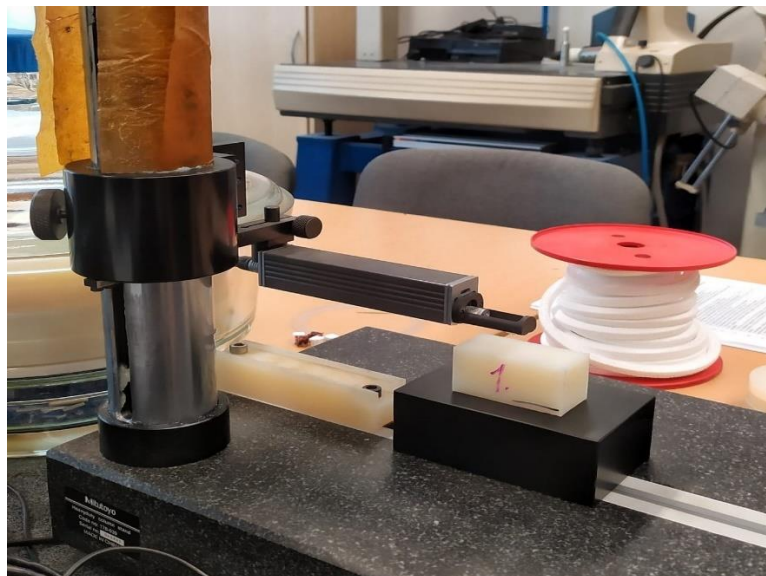


Figure 19: Polymer surface analysis with MITUTOYO measurement machine

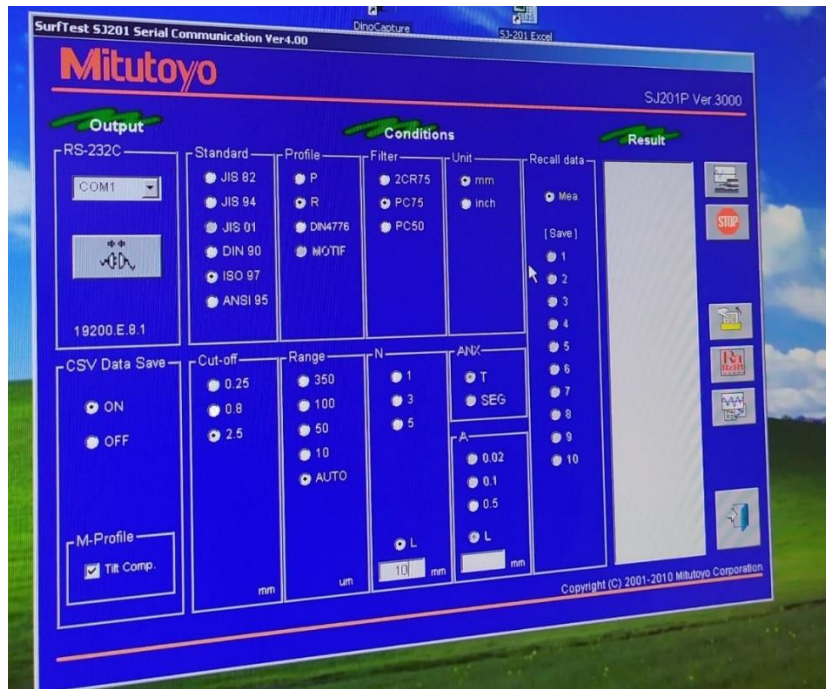


Figure 20: Visualization of the MITUTOYO SurfTest SJ201 Serial Communication Ver4.00 Analysis Program Interface

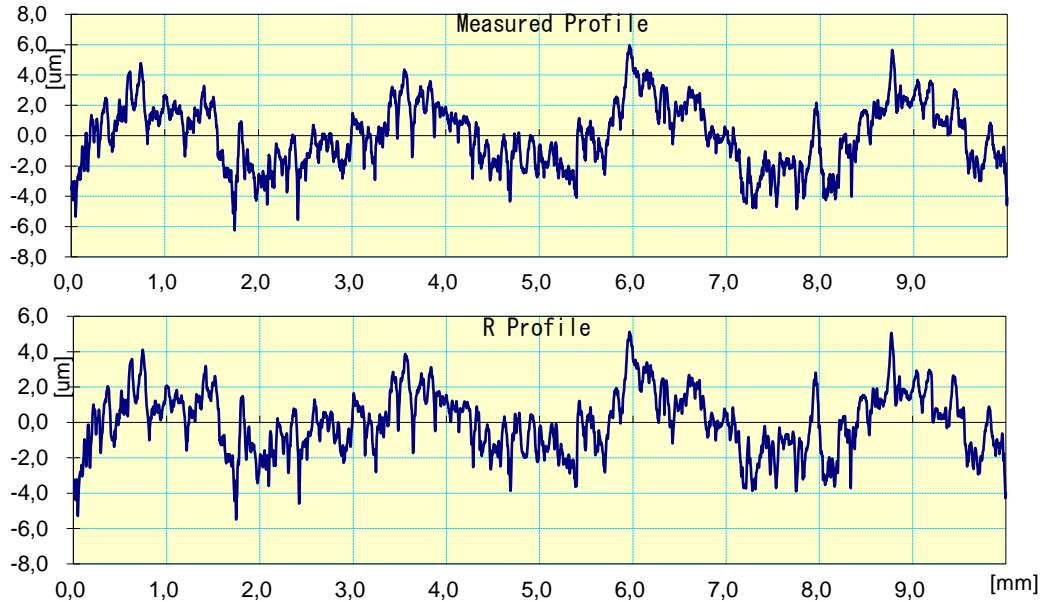
During the measurement process, I employed MITUTOYO's SurfTest SJ201 Serial Communication Ver4.00 application. Adhering to the ISO 97 Standard, I set the profile to R, filter to PC75, unit to mm, cut-off to 2.5, and range to auto. Additionally, I activated options for data recall, CSV data saving, and M profile completion. In section N, tests were conducted with a length of 10 mm. Each specimen underwent meticulous scrutiny, with three tests performed on its milled surface: one on the bottom left, one in the middle, and one on the top right. The resulting graphs and analyses were meticulously processed within the MITUTOYO application. The data extracted from the analysis are meticulously presented on the subsequent page. It is noteworthy that one of the critical aspects of this application lies in the exceptional precision of the measuring instrument utilized, which consequently provides highly reliable results.

7. RESULTS AND EVALUATION

7.1. PA66

Mitutoyo

CERTIFICATE OF INSPECTION



Work Name	PA66 First Test	Operator	Mitutoyo
Measuring Tool	SurfTest SJ-201	Comment	Ver4.00
Standard	ISO 1997	Evaluation length	10.0 mm
Profile	R	Cut-Off	2.5 mm
Range	AUTO	Filter	PC75
Ra	1.42 µm		
Ry	10.61 µm		
Rz	10.61 µm		
Rq	1.74 µm		

Figure 21: Example of the recorded sheet

The results of the Ra, Ry, Rz, and Rq values in surface roughness analysis using MITUTOYO's application SurfTest SJ201 Serial are displayed as seen in the Figure 21. Ra, Ry, Rz, and Rq are parameters utilized to quantify surface roughness. Ra, or average surface roughness, denotes the mean height of micro-roughness on a surface, with lower values indicating smoother surfaces. Ry, representing the maximum peak height, indicates the tallest peak on the surface, shows the height of the most prominent irregularities. Rz, or average maximum profile height, signifies the mean height of the tallest peaks in the surface profile, providing insight into the elevation of the highest points on the surface. Rq, the root mean square, reflects the square root of the average of the squares of all roughness values on the surface, offering a measure of the

overall surface irregularity. In the first of the three tests conducted on the white PA66 in the example, the values for Ra, Ry, Rz, and Rq are provided as 1.42 μm , 10.61 μm , 10.61 μm , and 1.74 μm , respectively, offering comprehensive information about the surface's average, maximum, and overall roughness characteristics.

Table 3: Surface Roughness values according to the matrix

PA66 (μm)		S1	S2	S3	AVERAGE
No.1	Ra	1,41	1,36	1,51	1,43 μm
	Ry	10,61	10,49	10,89	10,66 μm
	Rz	10,61	10,49	10,89	10,66 μm
	Rq	1,74	1,69	1,84	1,76 μm
No.2	Ra	1,5	1,68	1,75	1,64 μm
	Ry	10,5	11,87	12,87	11,75 μm
	Rz	10,5	11,87	12,87	11,75 μm
	Rq	1,81	2,03	2,12	1,99 μm
No.3	Ra	4,07	4,14	4,42	4,21 μm
	Ry	21,24	19,72	21,82	20,93 μm
	Rz	21,24	19,72	21,82	20,93 μm
	Rq	4,77	4,74	5,08	4,86 μm
No.4	Ra	0,71	0,79	0,93	0,81 μm
	Ry	6,57	7,05	7,85	7,16 μm
	Rz	6,57	7,05	7,85	7,16 μm
	Rq	0,9	1,01	1,17	1,03 μm
No.5	Ra	1,04	1,17	1,31	1,17 μm
	Ry	8,64	7,97	9,23	8,61 μm
	Rz	8,64	7,97	9,23	8,61 μm
	Rq	1,28	1,42	1,58	1,43 μm
No.6	Ra	1,46	1,51	1,54	1,50 μm
	Ry	10,11	8,15	9,54	9,27 μm
	Rz	10,11	8,15	9,54	9,27 μm
	Rq	1,77	1,79	1,84	1,80 μm
No.7	Ra	0,67	0,62	0,58	0,62 μm
	Ry	7,98	5,21	7,61	6,93 μm
	Rz	7,98	5,21	7,61	6,93 μm
	Rq	0,9	0,77	0,78	0,82 μm
No.8	Ra	0,99	0,94	1,05	0,99 μm
	Ry	8,21	7,21	7,88	7,77 μm
	Rz	8,21	7,21	7,88	7,77 μm
	Rq	1,25	1,16	1,31	1,24 μm
No.9	Ra	1,45	1,4	1,25	1,37 μm
	Ry	9,51	8,12	9,09	8,91 μm
	Rz	9,51	8,12	9,09	8,91 μm
	Rq	1,76	1,69	1,54	1,66 μm

PA66-GF30(μm)		S1	S2	S3	AVERAGE
No.1	Ra	1,27	1,29	1,31	1,29 μm
	Ry	12,74	17,25	15,93	15,31 μm
	Rz	12,74	17,25	15,93	15,31 μm
	Rq	1,65	1,72	1,73	1,70 μm
No.2	Ra	1,53	1,55	1,49	1,52 μm
	Ry	13,08	14,56	18,17	15,27 μm
	Rz	13,08	14,56	18,17	15,27 μm
	Rq	1,88	1,94	1,93	1,92 μm
No.3	Ra	3,95	3,7	4,26	3,83 μm
	Ry	25,23	23,38	29,37	25,99 μm
	Rz	25,23	23,38	29,37	25,99 μm
	Rq	4,62	4,34	4,91	4,62 μm
No.4	Ra	0,9	0,87	1	0,92 μm
	Ry	11,59	12,3	11,72	11,87 μm
	Rz	11,59	12,3	11,72	11,87 μm
	Rq	1,21	1,16	1,28	1,22 μm
No.5	Ra	1,26	1,26	1,26	1,26 μm
	Ry	13,25	12,51	18,36	14,71 μm
	Rz	13,25	12,51	18,36	14,71 μm
	Rq	16,5	1,61	1,73	1,67 μm
No.6	Ra	1,6	1,53	1,44	1,52 μm
	Ry	16,66	15,95	15,08	15,90 μm
	Rz	16,66	15,95	15,08	15,90 μm
	Rq	2,05	1,97	1,84	1,95 μm
No.7	Ra	0,78	0,8	0,84	0,81 μm
	Ry	10,78	9,52	11,21	10,50 μm
	Rz	10,78	9,52	11,21	10,50 μm
	Rq	1,1	1,09	1,12	1,10 μm
No.8	Ra	0,9	0,91	0,92	0,91 μm
	Ry	11,5	12,52	11,23	11,75 μm
	Rz	11,5	12,52	11,23	11,75 μm
	Rq	1,29	1,27	1,28	1,28 μm
No.9	Ra	1,45	1,57	1,39	1,47 μm
	Ry	13,54	15,27	13,21	14,01 μm
	Rz	13,54	15,27	13,21	14,01 μm
	Rq	1,87	2,06	1,77	1,90 μm

Table 3 (a) of the PA66 heading represents divisions from No.1 to No.9, indicating each sample of the PA66 polymer. As seen in No. 1, it is divided into four sections representing Ra, Ry, Rz, and Rq values. S1, S2, and S3 indicate that each section was analyzed three times. The unit

used for surface roughness is μm (micrometers). The Table 3 on the right side (b) displays the tests for the PA66-GF30 glass fiber polymer. All information applicable to the Table 3 on the left side is also valid for the Table 3 on the right side.

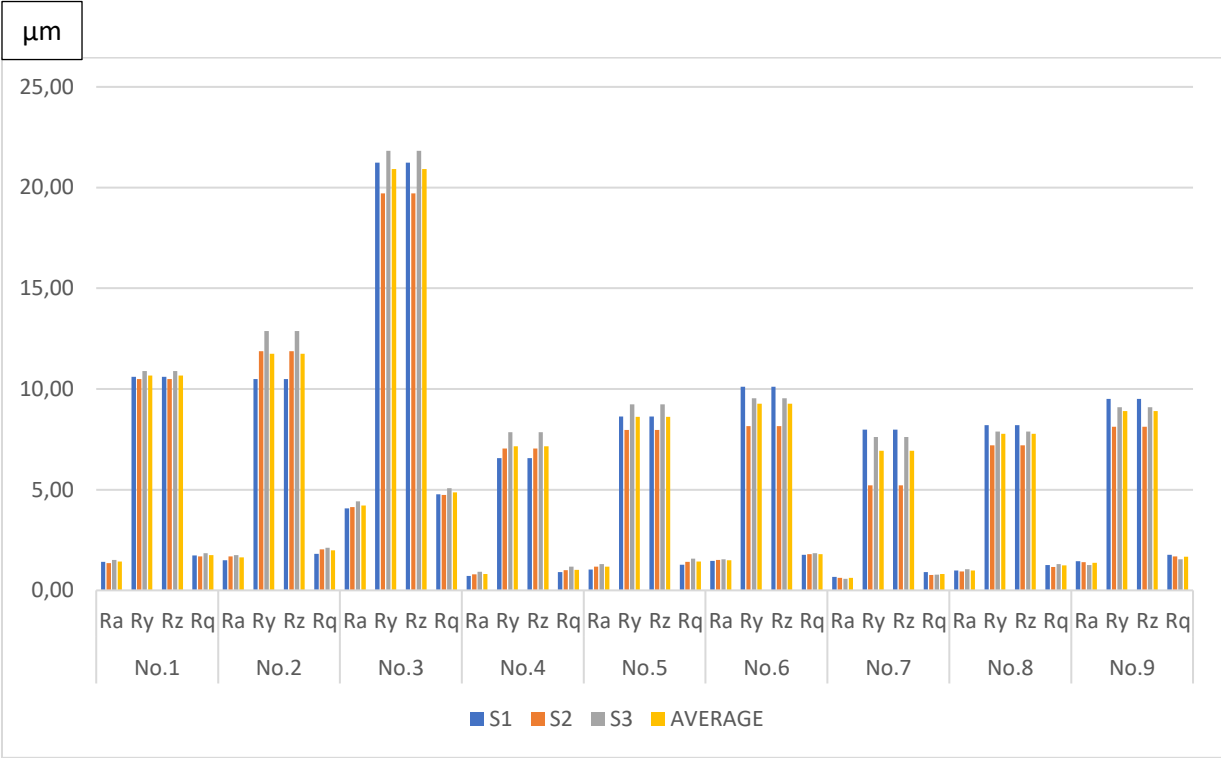


Figure 22: Measurement Results for Surface Roughness Parameters of PA 66 Test Samples

The Figure 22 presents the measurement results for the surface roughness parameters Ra, Rz, Ry, and Rq of PA 66 test samples. Numbered from 1 to 9, the test samples are measured on a vertical scale ranging from 0 to 25, with increments of 5. This scale provides a clear range for assessment. Each test sample undergoes three separate measurement processes named S1, S2, and S3 to ensure the reliability and consistency of the collected data. Additionally, the table includes an ‘Average’ column for each parameter, calculated from the values of S1, S2, and S3, offering a comprehensive summary of the surface roughness characteristics for each sample. I created this table to facilitate the understanding of the measurement results implications on the performance and applicability of the material in different engineering applications.

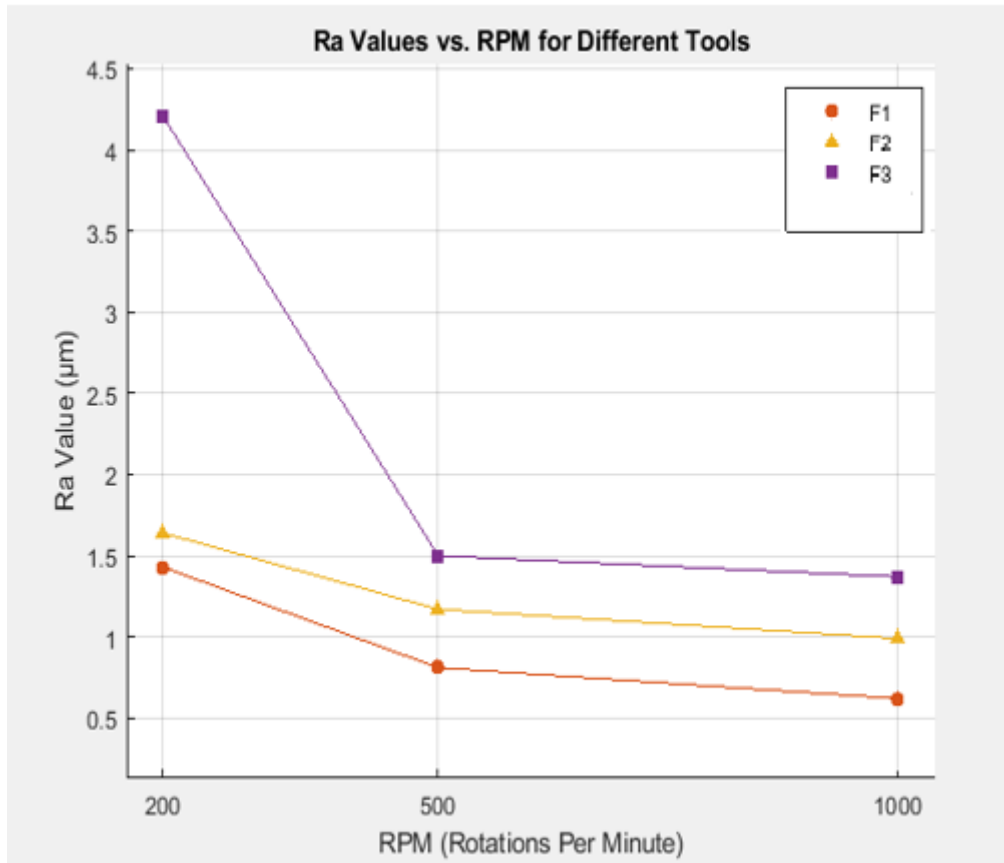


Figure 23: Ra Values vs. RPM of the tool for PA66

The Figure 23, illustrates the difference of the surface roughness parameter Ra for tool with different RPM settings. In the graph, RPM values are set at 200, 500, and 1000, representing three different cutting speed (rpm) while F1, F2, and F3 feed values. The connecting lines enhance the visualization of data trends between these points. The X-axis represents RPM (Rotations Per Minute), while the Y-axis indicates the Ra value (μm). As seen in the Figure 23, e.g under F1 an increase from 200 RPM to 500 RPM results in a change of Ra with -43.36%, and increasing the speed from 500 to 1000 the Ra decrease was -23.46% only, showing lower sensitivity for cutting speed change. These changes demonstrate that as RPM increases, surface roughness decreases, indicating the impact of machining speed on surface quality. Similarly, all the differences are expressed in Table 4.

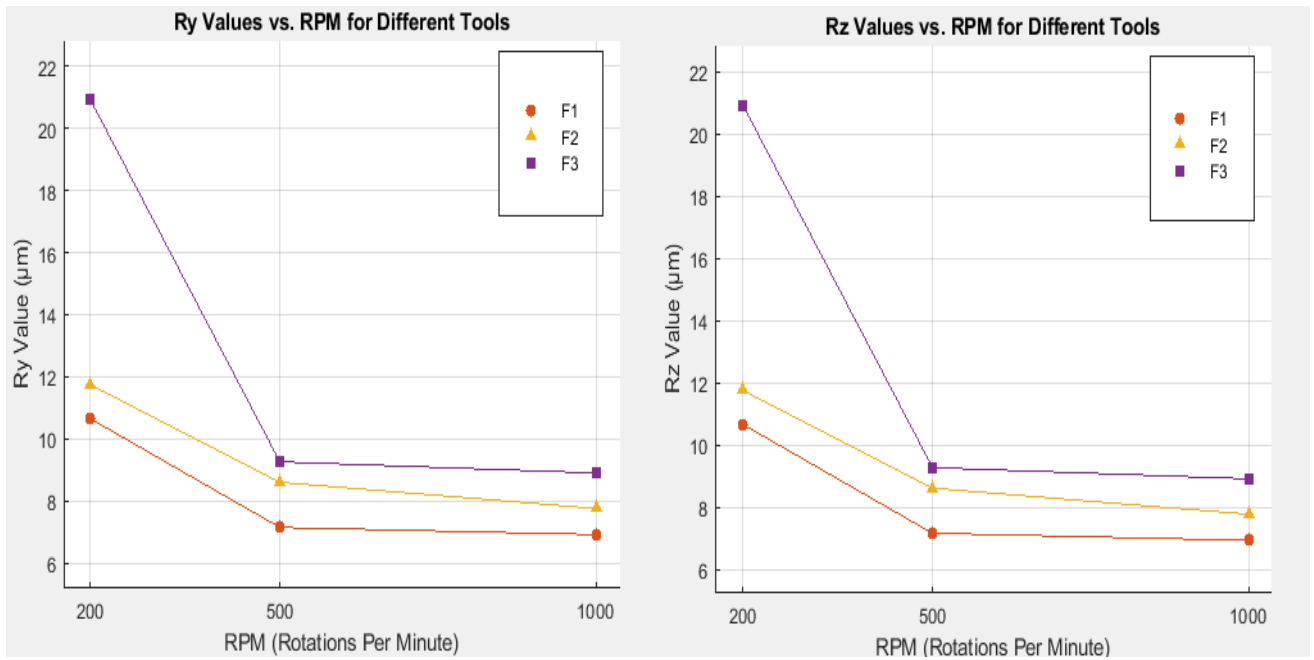


Figure 24: Ry and Rz Values vs. RPM of the tool for PA66

The Figure 24 shows the difference in surface roughness parameters, Ry and Rz, across different RPM settings for different parameters. Each set of RPM values – 200, 500, and 1000 – corresponds to three distinct parameters: Ry1, Ry2, and Ry3 for Ry, and F1, F2, and F3 for Rz. The scatter plots visually represent the measured values of each parameter at the specified RPM levels, while the connecting lines aid in identifying trends between these data points. The X-axis represents RPM (Rotations Per Minute), while the Y-axis indicates the Ry and Rz values (μm). Analysis reveals that transitioning from 200 RPM to 500 RPM results in decreases of -32.96% (Ry1), -26.64% (Ry2) for Ry, and similar trends are observed for Rz. Specifically, for Rz, transitioning from 200 RPM to 500 RPM results in decreases of -32.96% for F1, -26.64% for F2. Similarly, transitioning from 500 RPM to 1000 RPM shows decreases in Rz values of -3.21% for F1, -9.76% for F2. These observations provide insights into the effects of RPM settings on surface roughness parameters for different tools.

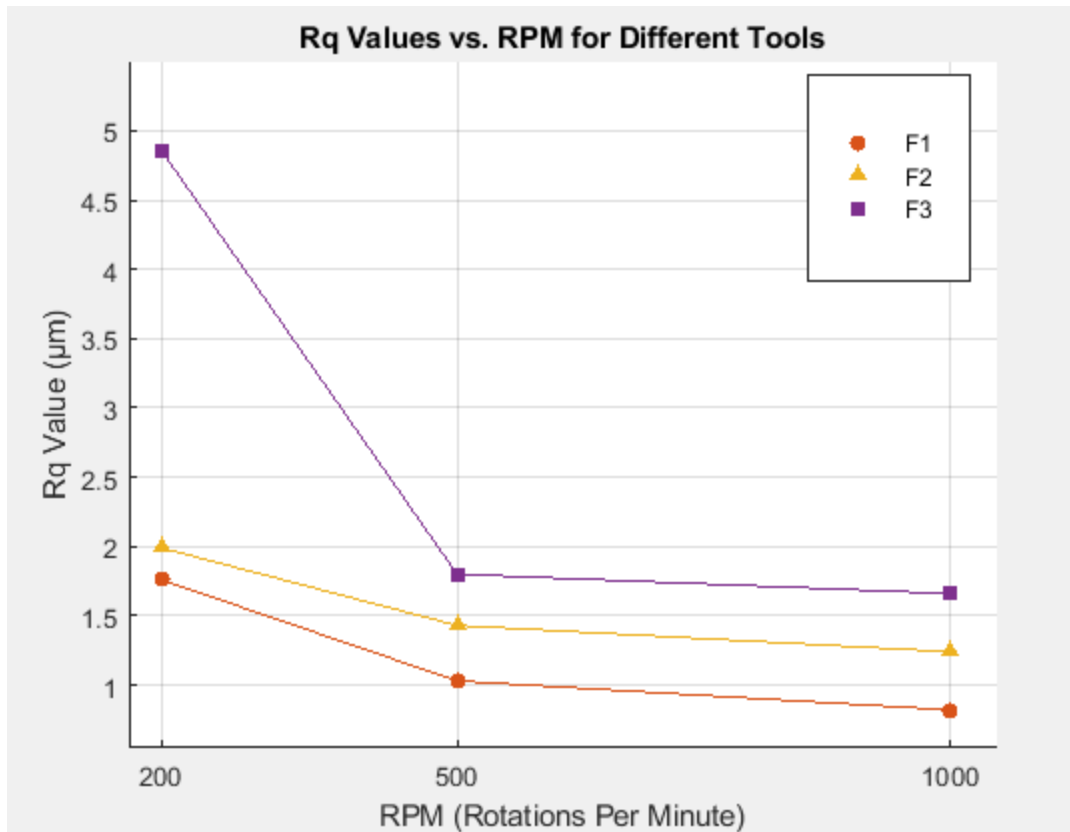


Figure 25: Rq Values vs. RPM of the tool for PA66

The Figure 25, shows the difference of the surface roughness parameter Rq for parameter with different RPM settings. In the graph, RPM values are set at 200, 500, and 1000, representing three different cutting speed (rpm) while F1, F2, and F3 feed values. The scatter plot visually represents the measurement results for each parameter at the specified RPM levels, while the connecting lines aid in identifying trends between these data points. The X-axis denotes the RPM (Rotations Per Minute), while the Y-axis indicates the Rq value (μm). Analysis of the provided data reveals that transitioning from 200 RPM to 500 RPM results in shifts of -41.48% (F1), -28.14% (F2) in Rq values. This observation suggests a correlation between increasing RPM and improved surface smoothness, underscoring the influence of machining speed on surface quality. Moreover, an increase from 500 RPM to 1000 RPM yields changes of -20.39% for F1, -13.29% for F2 indicating a diminishing effect of higher rotational speeds on surface roughness. Similarly, all the differences are expressed in Table 4.

Table 4: Surface Roughness Parameter Changes Across RPM Transitions for PA66 Material

PA66		200 rpm -->500 rpm	500 rpm -->1000 rpm
		$\Delta 1 = 150\%$	$\Delta 2 = 100\%$
ΔRa [%]	F1	-43,36%	-23,46%
	F2	-28,66%	-15,38%
	F3	-64,15%	-8,67%
ΔRy [%]	F1	-32,96%	-3,21%
	F2	-26,64%	-9,76%
	F3	-55,68%	-3,88%
ΔRz [%]	F1	-32,96%	-3,21%
	F2	-26,64%	-9,76%
	F3	-55,68%	-3,88%
ΔRq [%]	F1	-41,48%	-20,39%
	F2	-28,14%	-13,29%
	F3	-62,14%	-7,78%

The Table 4 thorough examination explores the changes in surface roughness metrics for PA66 material between several RPM transitions, specifically between 200 and 500 RPM and between 500 and 1000 RPM. After examining the table closely, it becomes evident that different percentage shifts occurred during these transitions. Firstly, the change from 200 to 500 RPM involves a significant increase in $\Delta 1$, signaling a substantial 150% change. In terms of surface roughness parameters, ΔRa showcases significant decreases of -43.36% (F1), -28.66% (F2), and -64.15% (F3) from 200 to 500 RPM, indicating a pronounced refinement in surface smoothness. Similarly, both ΔRy and ΔRz exhibit declines across all parameters, albeit with varying magnitudes. Concurrently, ΔRq mirrors this trend with reductions of -41.48% (F1), -28.14% (F2), and -62.14% (F3), elucidating a substantial enhancement in surface quality. However, during the transition from 500 to 1000 RPM, more subdued changes are observed across all parameters compared to the previous transition. Smaller decreases in ΔRa , ΔRy , ΔRz , and ΔRq suggest a diminishing effect of higher RPM on surface roughness parameters, indicative of a saturation point reached in the material's machining process.

Table 5: Feed Rate Effects on Surface Roughness Parameters at Different RPM Settings for PA66

Vertical analyses of Figs. 23-25, PA66		200 rpm	500 rpm	1000 rpm
$\Delta=F1-F2$	$\Delta1 R_a$ [%]	14.69	44.44	59.68
$\Delta=F2-F3$	$\Delta2 R_a$ [%]	156.71	28.21	38.38
$\Delta=F1-F2$	$\Delta1 R_y$ [%]	10.25	20.25	12.11
$\Delta=F2-F3$	$\Delta2 R_y$ [%]	77.63	7.66	14.65
$\Delta=F1-F2$	$\Delta1 R_z$ [%]	10.25	20.25	12.11
$\Delta=F2-F3$	$\Delta2 R_z$ [%]	77.63	7.66	14.65
$\Delta=F1-F2$	$\Delta1 R_q$ [%]	13.07	38.83	51.22
$\Delta=F2-F3$	$\Delta2 R_q$ [%]	143.22	25.87	33.87

Table 5 provides a thorough examination of the relationship between surface roughness (R_a) and feed rate differences for PA66 material in different RPM settings. At 200 RPM, transitioning from F1 to F2 results in a 14.69% increase in R_a , illustrating a shift towards rougher surfaces with higher feed rates, indicative of the direct effect of feed rate adjustments have on surface quality at lower speeds. This trend intensifies with a 156.71% leap in R_a when moving from F2 to F3, shows the how important of feed rate in surface finish degradation at lower RPMs. As speeds increase to 500 RPM, the R_a increase from F1 to F2 is 44.44%, suggesting that higher RPMs moderate but do not eliminate the influence of feed rate changes on roughness. The progression to 1000 RPM further evolves this relationship; the R_a increase from F1 to F2 jumps to 59.68%, and from F2 to F3 to 38.38%, underscoring a diminishing sensitivity to feed rate adjustments at higher speeds. Higher speeds generally reduce roughness.

7.2. PA66-GF30

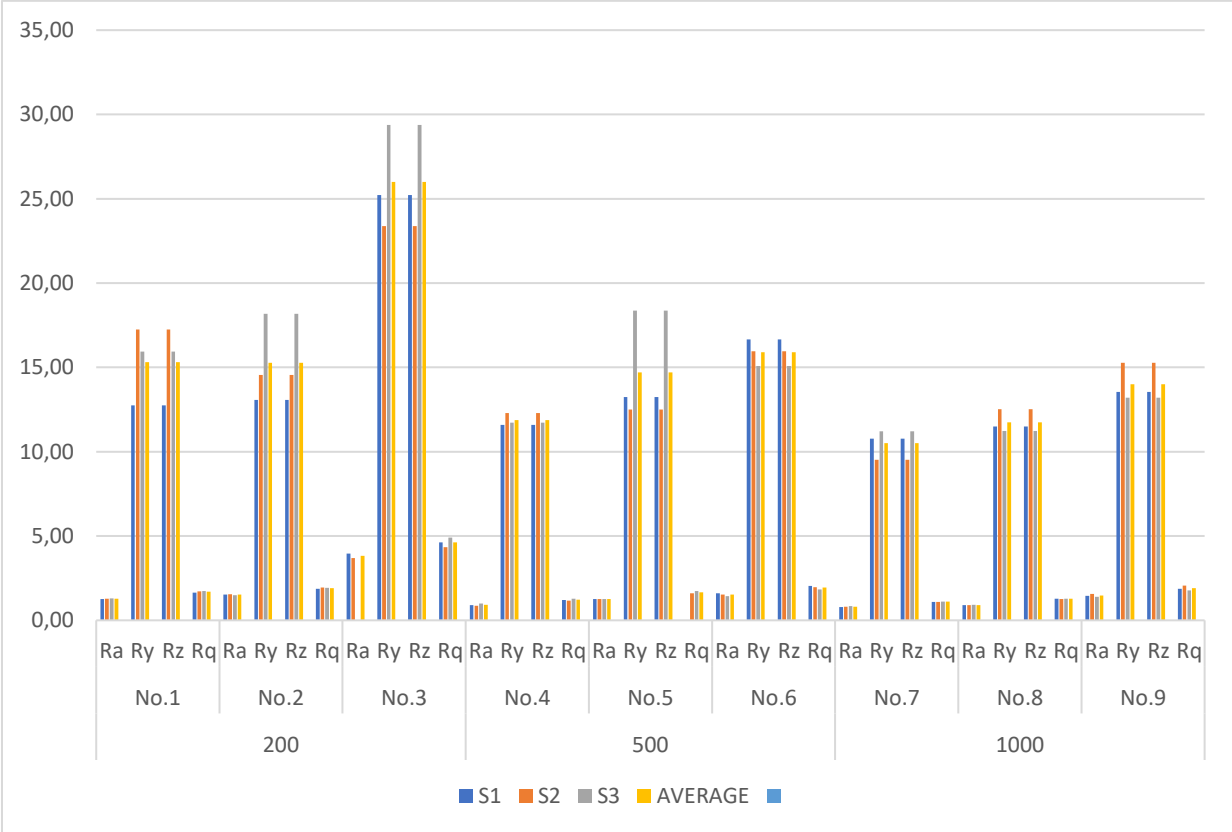


Figure 26: Measurement Results for Surface Roughness Parameters of PA66-GF30 Test Samples

Figure 26 shows the measurement results for surface roughness parameters Ra, Rz, Ry, and Rq of PA66-GF30 polymer test samples. Numbered from 1 to 9, these samples are measured on a vertical scale ranging from 0 to 35, with increments of 5, emphasizing the surface characteristics. Each test sample undergoes three separate measurement processes, denoted as S1, S2, and S3, to ensure data reliability and consistency. Additionally, an ‘Average’ column is included for each parameter, derived from the values of S1, S2, and S3, providing a comprehensive summary of surface roughness for each sample. I created this table to facilitate the understanding of the measurement results implications on the performance and applicability of the material in different engineering applications.

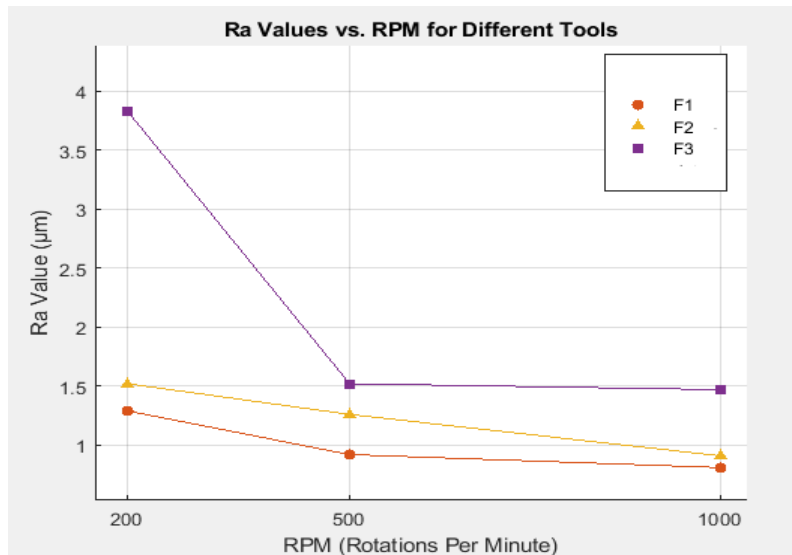


Figure 27: Ra Values vs. RPM of the tool for PA66-GF30

As it was already noted, when comparing the Ra values for PA66-GF30 in Figure 27 to those for PA66 in Figure 23, changing the RPM from 200 to 500 in PA66-GF30 causes the Ra to change by -28.68%. Followed by a -11.96% reduction with increase to 1000 RPM, indicating reduced sensitivity to cutting speed changes compared to natural PA66. Conversely, for natural PA66, the same RPM transition leads to a more substantial decrease in Ra by -43.36%, with an additional -23.46% reduction from 500 to 1000 RPM, demonstrating higher responsiveness to machining speed adjustments. This comparison shows how the addition of glass fibers in PA66 diminishes its reactivity to surface quality improvements achievable at higher cutting speeds. Similarly, all the differences are expressed in Table 6.

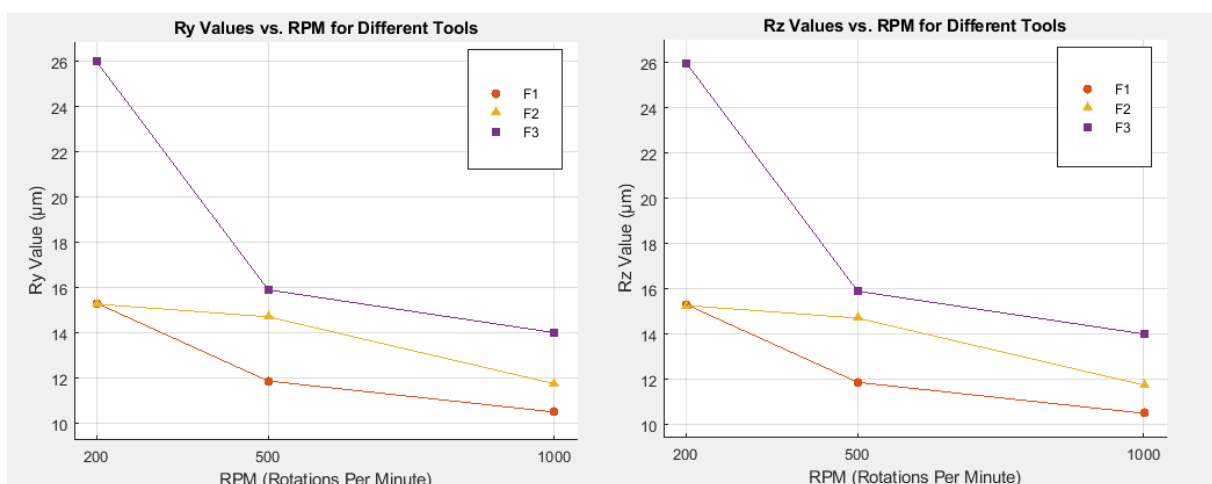


Figure 28: Ry and Rz Values vs. RPM of the tool for PA66-GF30

As previously observed, when comparing the results of PA66-GF Ra in Figure 28 with those in Figure 24, it is evident that transitioning from 200 to 500 RPM in PA66 resulted in a notable

decrease in surface roughness (Ry and Rz), with reductions of -22.45% and -3.66%, respectively. However, under the same conditions, these reductions were less pronounced for PA66-GF30, with decreases of -11.54% for Ry and -20.11% for Rz. This disparity can be attributed to the presence of glass fibers in PA66-GF30, which enhance the material's stiffness and influence its behavior during machining. Consequently, they mitigate the impact of faster cutting speeds on surface finish improvement. In essence, the inclusion of glass fibers in PA66-GF30 diminishes the influence of RPM on the observed improvements in surface roughness seen in natural PA66.

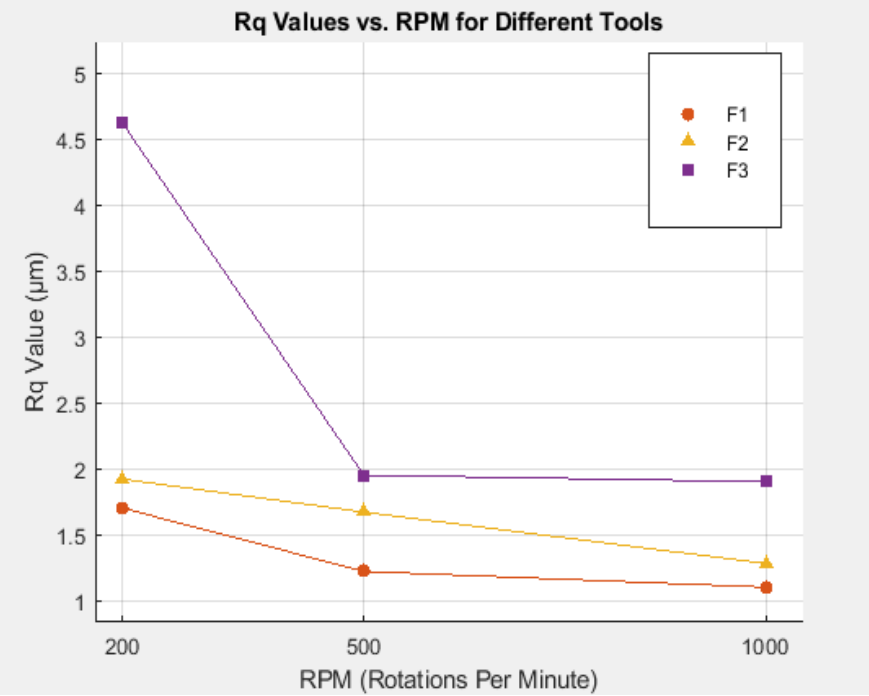


Figure 29: Rq Values vs. RPM of the tool for PA66-GF30

The comparison of Rq results between PA66-GF30 in Figure 29 and PA66 in Figure 25 highlights significant differences. When transitioning from 200 RPM to 500 RPM, PA66-GF30 showed a decrease of -28.24% (F1), -13.02% (F2) in Rq values, whereas natural PA66 exhibited a more pronounced reduction under the same conditions, with a decrease of -41.48% (F1), -28.14% (F2). The lower susceptibility of PA66-GF30 to changes in RPM suggests that alterations in the material's mechanical properties, particularly during the transition to higher rotational speeds, have a diminished effect on surface finish.

Table 6: Surface Roughness Parameter Changes Across RPM Transitions for PA66-GF30
Material

PA66-GF30		200 rpm -->500 rpm	500 rpm -->1000 rpm
		$\Delta 1 =150\%$	$\Delta 2 =100\%$
ΔRa [%]	F1	-28,68	-11,96
	F2	-17,11	-27,78
	F3	-60,36	-3,29
ΔRy [%]	F1	-22,45	-11,54
	F2	-3,66	-20,11
	F3	-38,91	-11,88
ΔRz [%]	F1	-22,45	-11,54
	F2	-3,66	-20,11
	F3	-38,91	-11,88
ΔRq [%]	F1	-28,24	-9,84
	F2	-13,02	-23,35
	F3	-57,83	-2,56

Based on the data in Table 6, it is evident that there are notable differences in surface roughness metrics between PA66 and PA66-GF30 materials. Particularly, during the transition from 200 to 500 RPM, the reductions in ΔRa , ΔRy , and ΔRz values for PA66-GF30 are observed to be more moderate compared to PA66. For instance, while PA66-GF30 experiences decreases of -28.68% (F1), -17.11% (F2), and -60.36% (F3) in ΔRa , PA66 exhibits higher reductions of -43.36% (F1), -28.66% (F2), and -64.15% (F3), respectively. Similarly, during the transition from 500 to 1000 RPM, the changes in surface roughness parameters for PA66-GF30 are more limited compared to PA66. These results indicate that adding glass fiber reinforcement significantly affects how the material responds to improvements in surface quality during machining.

Table 7: Feed Rate Effects on Surface Roughness Parameters at Different RPM Settings for PA66-GF30

Vertical analyses of Figs. 23-25, PA66-GF30		200 rpm	500 rpm	1000 rpm
$\Delta=F1-F2$	$\Delta1 R_a$ [%]	17.83	36.96	12.35
$\Delta=F2-F3$	$\Delta2 R_a$ [%]	152.63	20.63	61.54
$\Delta=F1-F2$	$\Delta1 R_y$ [%]	0.26	23.91	11.90
$\Delta=F2-F3$	$\Delta2 R_y$ [%]	69.89	8.11	19.06
$\Delta=F1-F2$	$\Delta1 R_z$ [%]	0.26	23.91	11.90
$\Delta=F2-F3$	$\Delta2 R_z$ [%]	69.89	8.11	19.06
$\Delta=F1-F2$	$\Delta1 R_q$ [%]	13	36.07	16.36
$\Delta=F2-F3$	$\Delta2 R_q$ [%]	140.63	16.77	48.44

Table 7 presents an in-depth analysis of the relationship between surface roughness (R_a) and feed rate shifts for PA66-GF30 material across different RPM settings. R_a increases 17.83% at 200 RPM when switching from F1 to F2, suggesting a move toward higher feed rates and rougher surfaces, as seen in PA66. In contrast to PA66, the percentage increase in R_a is smaller. With a R_a increase of 152.63% when going from F2 to F3, which is also less than the corresponding increase in PA66, the trend becomes more pronounced at higher feed rates. The R_a increases from F1 to F2 and from F2 to F3 are also lower for PA66-GF30 compared to PA66 as speeds rise to 500 RPM and 1000 RPM, suggesting a decreased sensitivity to feed rate adjustments at higher speeds. These findings imply that, in comparison to PA66, PA66-GF30 shows less pronounced changes in surface roughness in response to changes in feed rate. This difference is probably caused by variations in the mechanical and compositional characteristics of the two materials.

8. COMPARISON OF SURFACE RESULTS

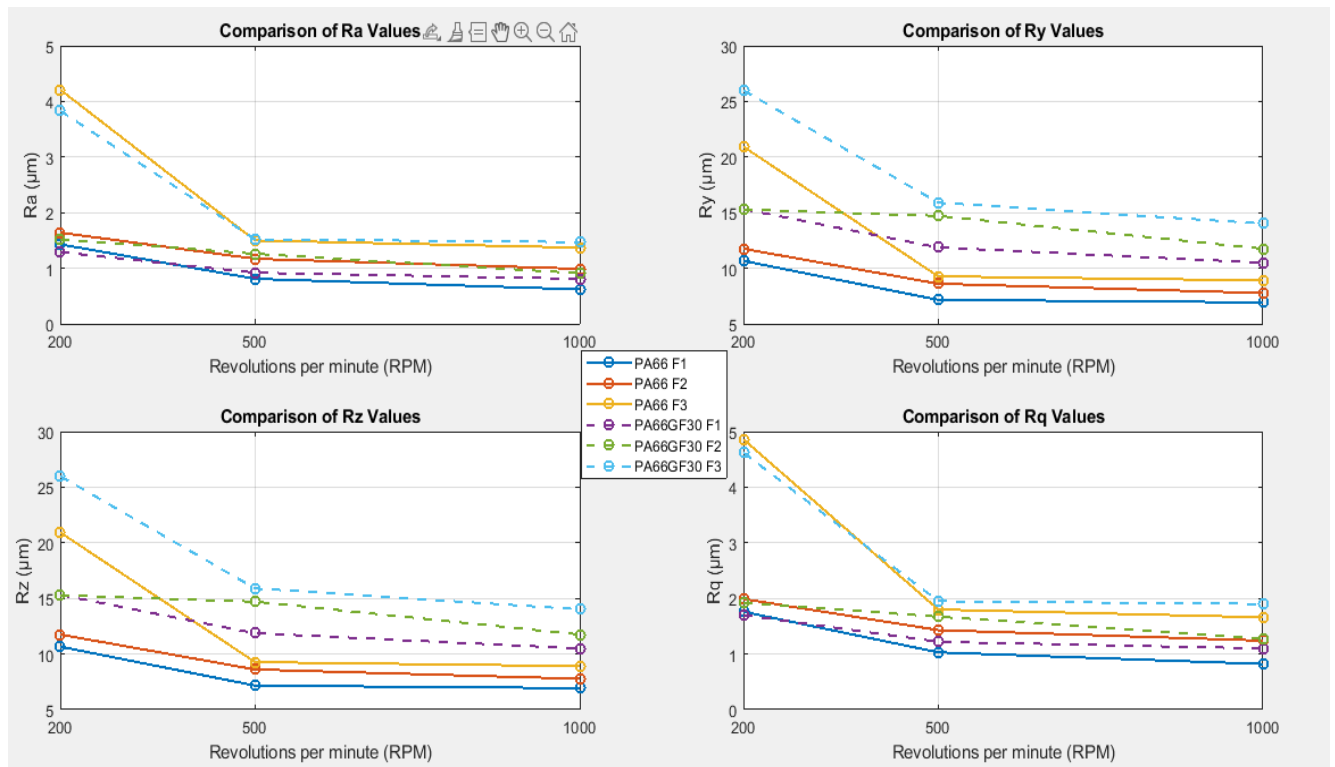


Figure 29: Comparison of Surface Roughness Parameters for PA66 and PA66GF30

Figure 29 contains a comprehensive comparison of PA66 and PA66-GF30. In the comparisons, PA66 has an average Ra value of 1.43 μm , while PA66-GF30 has an average Ra value of 1.29 μm . This shows that glass fiber reinforcement reduces the surface roughness of PA66-GF30, resulting in a smoother surface.

Similarly, when Ry, Rz and Rq values are analyzed, PA66-GF30 polymer has lower values in terms of surface smoothness. So I can say that glass fibers do a better job at high cutting speeds. However, as an exception, when I examine the Ry values, it is seen that the average values for PA66 are 10.66 μm while the average values for PA66-GF30 are 15.31 μm . This shows that the addition of glass fiber reinforcement affects the surface roughness of the material in some cases. This means that the PA66-GF30 polymer has higher strength properties and in some cases outperforms behind PA66 in terms of surface roughness (Ry parameter results of PA66-GF).

There are also differences in the comparisons made according to RPM values. For example, while PA66 shows a significant sudden decrease in Ra values as RPM values increase, similarly, this decrease in Ra values is more limited for PA66-GF30. At the transition from 200 RPM to 500 RPM, the PA66 exhibits a 43.36% decrease in Ra values, while this decrease to 28.68% in

the PA66-GF30. Similarly, during the transition from 500 RPM to 1000 RPM, PA66 has a more abrupt transition, while PA66-GF30 does not show a significant decrease.

When the effect of feed rate is analyzed, differences are observed in the effect on surface roughness between PA66 and PA66-GF30 at different RPM settings. For example, for $\Delta=F1-F2$ at 200 RPM for PA66 (F1 to F2 for PA66) there is a 14.69% increase in Ra values, while the same transition (F1 to F2 for PA66-GF30) results in a 17.83% increase for PA66-GF30. This shows that the addition of glass fiber reinforcement changes the behavior of the material during processing.

9. CONCLUSION

In conclusion, there have been many studies on natural PA66 and PA66-GF30, but there is not enough detailed information about how cutting parameters can influence the surface roughness parameters.

All this data shows that PA66 and PA66-GF30 have different advantages and disadvantages. PA66 has a wider range of applications than PA66-GF30 due to its lower price and ease of processing; however, PA66-GF30 offers properties such as lower surface roughness and higher mechanical strength, which encourages the manufacturer to choose a material suitable for the area in which it will be used.

On close inspection, it is clearly seen that the incorporation of glass fiber reinforcement into PA66 polymer causes a remarkable reduction in surface roughness, making it smoother than natural PA66. It is also observed that PA66-GF30 exhibits decreasing values for parameters such as Ry, Rz and Rq, indicating an increasing surface roughness. However, it should be noted that the introduction of glass fiber can sometimes lead to increased surface roughness, as seen in the comparison of Ry values.

From here, it can be concluded that when examining the Surface Roughness Parameter Changes Across RPM transitions for PA66-GF30 material table (Table 6), I observe that there are abrupt changes in the parameters for milling applications of PA66-GF30, indicating that the application of glass fiber to polymers causes sudden and sharp changes in surface roughness, leading to higher levels of uncertainty and unpredictability.

However, when I examine the Surface Roughness Parameter Changes due to RPM transitions table (Table 4) for PA66 material, I see that the parameters and the results obtained are closer to each other and it is easier to predict how the surface roughness of the polymer will react than

PA66-GF30. This shows that PA66 has higher predictability and lower uncertainty and is easier to predict than PA66-GF30 due to the similarity of the parameters and results.

Moreover, when comparing the RPM values, it can be noticed that PA66 experiences more pronounced reductions in Ra values as the RPM increases. This suggests that PA66-GF30 is less sensitive to changes in processing speed, which is probably due to the effect of glass fiber reinforcement.

Finally, the differences in the effect of feed rate on surface roughness between PA66 and PA66-GF30 across different RPM settings shows how the addition of glass fiber reinforcement alters the material's behavior.

10. SUMMARY

In summary, this thesis covers the results of an investigation to reveal the effect of milling technological settings on the surface properties of natural and glass reinforced PA66 plates. First, an overview of PA66 and PA66-GF30 materials is given. Then, the tools used and the testing process are described in detail. The materials used in the tests are PA66 and PA66-GF30 polymers reinforced with glass fiber. The 2D surface roughness parameters (Ra, Rz, Rq, Ry) of the two different materials are compared and analyzed. The effect of cutting speed and feed rate on the surface parameters was evaluated and the sensitivity of the materials to cutting speed and feed rate was observed.

At the beginning, the test specimens were precision cut using a manual cutting machine with water-based emulsion cooling. Milling was performed on a MAS brand milling machine with a milling cutter with a cutting diameter of 63 mm. The experiment involved varying spindle speeds (200, 500, 1000 rpm) and feed rates (100, 290, 790 mm/min) while maintaining a consistent depth of cut at 1.5 mm. Surface roughness was measured after milling using a MITUTOYO 178-039 SURFTEST SJ-400 series, taking measurements at three different points on each sample to provide comprehensive and reliable data.

The addition of glass fiber reinforcement to PA66 polymer leads to a significant reduction in surface roughness, leading to a reduction in surface smoothness compared to natural PA66. However, the addition of glass fiber can lead to an increase in surface roughness with abrupt changes in some parameters. This implies higher levels of uncertainty and unpredictability. For the natural PA66 polymer, the parameters and the results obtained are closer to each other and it is easier to predict how the surface roughness of the natural PA66 polymer will react.

Comparison of the RPM values shows that PA66 experiences more pronounced reductions in Ra values as RPM increases. This indicates that PA66-GF30 is less sensitive to changes in machining speed, possibly due to the effect of glass fiber reinforcement. The differences in the effect of feed rate on surface roughness between PA66 and PA66-GF30 at different RPM settings showed how the addition of glass fiber reinforcement changes the behavior of the material.

References

- Abdul Shukor, J., Said, S., Harun, R., Husin, S., & Kadir, Ab. (2016). Optimising of machining parameters of plastic material using Taguchi method. *Advances in Materials and Processing Technologies*, 2(1), 50–56.
<https://doi.org/10.1080/2374068x.2016.1143216>
- Anjaneyulu, B., Nagamalleswara Rao, G., Prahlada Rao, K., & Harshavardhan, D. (2017). Analysis of Process Parameters in Milling of Glass Fibre Reinforced Plastic Composites. *International Journal of Mechanical Engineering and Technology (IJMET)*, 8(2), 149–159.
- Arif, M. F., Saintier, N., Meraghni, F., Fitoussi, J., Chemisky, Y., & Robert, G. (2014). Multiscale fatigue damage characterization in short glass fiber reinforced polyamide-66. *Composites Part B: Engineering*, 61, 55–65.
<https://doi.org/10.1016/j.compositesb.2014.01.019>
- Bayraktar, S., & Turgut, Y. (2016). Investigation of the cutting forces and surface roughness in milling carbon-fiber-reinforced polymer composite material. *Materiali in Tehnologije*, 50(4), 591–600.
<https://doi.org/10.17222/mit.2015.199>
- Chiles, V., Black, S., Lissaman, A., & Martin, S. (1996). *Principles of engineering manufacture. (Third edition)*. Butterworth-Heinemann.
- Crowson, R. J., & Folkes, M. J. (1980). Rheology of short glass fiber-reinforced thermoplastics and its application to injection molding. II. The effect of material parameters. *Polymer Engineering and Science*, 20(14), 934–940.
<https://doi.org/10.1002/pen.760201404>
- Dobrocký, D., Sedlák, J., Joska, Z., Procházka, J., Studený, Z., & Pokorný, Z. (2021). Influence of Machining Parameters on the Surface Quality of Technical Plastics. *ECS Transactions*, 105(1), 381–389.
<https://doi.org/10.1149/10501.0381ecst>

- Edwards, K. L. (1998). An overview of the technology of fibre-reinforced plastics for design purposes. *Materials & Design*, 19(1-2), 1–10.
[https://doi.org/10.1016/s0261-3069\(98\)00007-7](https://doi.org/10.1016/s0261-3069(98)00007-7)
- Ghalme, S., Mankar, A., & Bhalerao, Y. J. (2016). Parameter optimization in milling of glass fiber reinforced plastic (GFRP) using DOE-Taguchi method. *SpringerPlus*, 5(1).
<https://doi.org/10.1186/s40064-016-3055-y>
- Hessman, P. A., Riedel, T., Welschinger, F., Hornberger, K., & Böhlke, T. (2019). Microstructural analysis of short glass fiber reinforced thermoplastics based on x-ray micro-computed tomography. *Composites Science and Technology*, 183, 107752.
<https://doi.org/10.1016/j.compscitech.2019.107752>
- Horst, J. J., & Spoomaker, J. L. (1996). Mechanisms of fatigue in short glass fiber reinforced polyamide 6. *Polymer Engineering and Science*, 36(22), 2718–2726.
<https://doi.org/10.1002/pen.10671>
- Izamshah, R., Azam, M. A., Hadzley, M., Ali, M. A. M., Kasim, M. S., & Aziz, M. S. A. (2013). Study of Surface Roughness on Milling Unfilled-polyetheretherketones Engineering Plastics. *Procedia Engineering*, 68, 654–660.
<https://doi.org/10.1016/j.proeng.2013.12.235>
- Kalácska, G. (2020) Tribology lecture ppt. MATE
- Khairusshima, M. K., Aqella, A.K. , & Sharifah, I.S.S. (2017). Optimization of Milling Carbon Fibre Reinforced Plastic Using RSM. *Procedia Engineering*, 184, 518–528.
<https://doi.org/10.1016/j.proeng.2017.04.122>
- Laun, H. M. (1984). Orientation effects and rheology of short glass fiber-reinforced thermoplastics. *Colloid and Polymer Science*, 262(4), 257–269.
<https://doi.org/10.1007/bf01410464>
- Lee, L. H. (1969). Strength -Composition relationships of random short glass fiber - thermoplastics composites. *Polymer Engineering and Science*, 9(3), 213–224.
<https://doi.org/10.1002/pen.760090310>
- Logins, A., & Torims, T. (2015). The Influence of High-speed Milling Strategies on 3D Surface Roughness Parameters. *Procedia Engineering*, 100, 1253–1261.
<https://doi.org/10.1016/j.proeng.2015.01.491>

- Masuelli, M. A. (2014). *Fiber reinforced polymers - the technology applied for concrete repair*. Intech.
- Oktem, H., Erzurumlu, T., & Erzincanli, F. (2006). Prediction of minimum surface roughness in end milling mold parts using neural network and genetic algorithm. *Materials & Design*, 27(9), 735–744.
<https://doi.org/10.1016/j.matdes.2005.01.010>
- Pecat, O., Rentsch, R., & Brinksmeier, E. (2012). Influence of Milling Process Parameters on the Surface Integrity of CFRP. *Procedia CIRP*, 1, 466–470.
<https://doi.org/10.1016/j.procir.2012.04.083>
- Prashanth, S., Subbaya, K., Nithin, K., & Sachhidananda, S. (2017). Fiber Reinforced Composites - A Review. *Journal of Material Science & Engineering*, 06(03).
<https://doi.org/10.4172/2169-0022.1000341>
- Santrach, D. (1982). Industrial applications and properties of short glass fiber-reinforced plastics. *Polymer Composites*, 3(4), 239–244.
<https://doi.org/10.1002/pc.750030410>
- Saptaji, K., Subbiah, S., & Dhupia, J. S. (2012). Effect of side edge angle and effective rake angle on top burrs in micro-milling. *Precision Engineering*, 36(3), 444–450.
<https://doi.org/10.1016/j.precisioneng.2012.01.008>
- Sorrentino, L., & Turchetta, S. (2011). "Milling of carbon fiber-reinforced plastics: analysis of cutting forces and surface roughness." 18th International Conference of Composite Materials.
- Uchiyama, R., Inoue, Y., Uchiyama, F., & Matsumura, T. (2021). Optimization in Milling of Polymer Materials for High Quality Surfaces. *International Journal of Automation Technology*, 15(4), 512–520.
<https://doi.org/10.20965/ijat.2021.p0512>
- Wang, F., Li, Y., Zhang, B., Jiang, F., Yang, L., & Lin, Y. (2021). Influence of process parameters on material removal during surface milling of curved carbon fiber-reinforced plastic (CFRP) components: evaluated by a novel residual height calculation method. *The International Journal of Advanced Manufacturing Technology*, 116(11-12), 3405–3415.
<https://doi.org/10.1007/s00170-021-07590-6>
- Wu, Z., Buck, D., Dong, J., Guo, X., Cao, P., & Zhu, Z. (2022). Investigation on Milling Quality of Stone–Plastic Composite Using Response Surface Methodology. *JOM*, 74(5), 2063–2070. <https://doi.org/10.1007/s11837-021-05024-y>

<https://www.assemblymag.com/articles/94868-boosting-performance-without-breaking-the-bank> (05/02/2024)

www.alformet.com/composite/frp/gfrp (13/10/2023)

<https://www.harveyperformance.com/in-the-loupe/depth-of-cut/> (15/10/2023)

<https://www.archcuttingtools.com/product/05000/> (08/11/2023)

<https://en.yeongyih.com.tw/cylindrical-milling-cutter.htm> (14/11/2023)

<https://www.sciencedirect.com/topics/engineering/end-mill> (24/11/2023)

<https://www.curbellplastics.com/services-capabilities/fabrication-machined-parts/plastic-machining-guidelines/> (10/02/2024)

<https://www.mcam.com/en/support/machinists-toolkit> (08/02/2024)

<https://www.boedeker.com/Technical-Resources/Technical-Library/Plastic-Machining-Guidelines> (03/02/2024)

List of Figures

Figure 1: Internal structure of engineering thermoplastic	6
Figure 2: Skin–shell–transition–core microstructure formation of PA66	8
Figure 3: Glass fiber reinforced polymer.....	9
Figure 4: Depth of cut visual expression.....	10
Figure 5: Solid carbide end mill with different helix angles	12
Figure 6: Cutting angle edge outer surface cutting diagram	12
Figure 7: Micrographs of specimens machined at different temperatures	13
Figure 8: Micrographs of specimens with different fiber orientations	15
Figure 9: Standard Type Straight-Tooth Cutter	17
Figure 10: Cylindrical Milling Cutters	18
Figure 11: Tool morphologies of the ball-end mill bits	19
Figure 12: End mill cutter geometry	20
Figure 13: Variety of surface roughness indicators and typical calculations	22
Figure 14: Photograph of cutting machine	24
Figure 15: Photograph of the polymers after the cutting process	25
Figure 16: Photograph of the polymers during the milling process	26
Figure 17: Fixation of polymers by using clamps in the machining centre.....	27
Figure 18: Photographs of the milling tool.....	27
Figure 19: Polymer surface analysis with MITUTOYO measurement machine.....	28
Figure 20: Visualization of the MITUTOYO Surftest SJ201 Serial Communication Ver4.00 Analysis Program Interface	29
Figure 21: Example of the recorded sheet	30
Figure 22: Measurement Results for Surface Roughness Parameters of PA 66 Test Samples	32
Figure 23: Ra Values vs. RPM of the tool for PA66.....	33
Figure 24: Ry and Rz Values vs. RPM of the tool for PA66	34
Figure 25: Rq Values vs. RPM of the tool for PA66	35
Figure 26: Measurement Results for Surface Roughness Parameters of PA66-GF30 Test Samples ...	38
Figure 27: Ra Values vs. RPM of the tool for PA66-GF30	39
Figure 28: Ry and Rz Values vs. RPM of the tool for PA66-GF30.....	39
Figure 29: Rq Values vs. RPM of the tool for PA66-GF30	40
Figure 29: Comparison of Surface Roughness Parameters for PA66 and PA66GF30	43

List of Tables:

Table 1: The Table of Spindle Speed and Feed Rate Values for Testing	25
Table 2: Tool parameters	28
Table 3: Surface Roughness values according to the matrix	31
Table 4: Surface Roughness Parameter Changes Across RPM Transitions for PA66 Material.....	36
Table 5: Feed Rate Effects on Surface Roughness Parameters at Different RPM Settings for PA66...	37
Table 6: Surface Roughness Parameter Changes Across RPM Transitions for PA66-GF30 Material .	41
Table 7: Feed Rate Effects on Surface Roughness Parameters at Different RPM Settings for PA66-GF30.....	42

DECLARATION

on authenticity and public assess of thesis

Student's name: Ferhat Furkan MAROL
Student's Neptun ID: BH57C4
Title of the document: Surface roughness analysis milled polymers
Year of publication: 2024
Department: Technical Institute

I declare that the submitted thesis is my own, original individual creation. Any parts taken from an another author's work are clearly marked, and listed in the table of contents.


If the statements above are not true, I acknowledge that the Final examination board excludes me from participation in the final exam, and I am only allowed to take final exam if I submit another thesis.

Viewing and printing my submitted work in a PDF format is permitted. However, the modification of my submitted work shall not be permitted.

I acknowledge that the rules on Intellectual Property Management of Hungarian University of Agriculture and Life Sciences shall apply to my work as an intellectual property.

I acknowledge that the electric version of my work is uploaded to the repository system of the Hungarian University of Agriculture and Life Sciences.

Place and date: Gödöllő 2024 year 04 month 17 day


Student's signature

DECLARATION

As a supervisor of Ferhat Furkan Marol (BH57C4), I declare that I have reviewed the final thesis and that I have informed the student of the requirements, legal and ethical rules for the correct handling of literary sources.

I recommend / do not recommend¹ the final thesis to be defended in the final examination.

The thesis contains a state or official secret: yes no^{*2}

Date: 2024 year April month 17 day



supervisor

TECHNICAL INSTITUTE
BACHELOR
Machine Production Technologies
THESIS

FERHAT FURKAN MAROL (BH57C4)

for

Title of the diploma thesis: Surface roughness analysis milled polymers

Given laboratory process

Task reference:

This thesis investigates the effects of different processing parameters on the surface roughness of PA66 and PA66-GF30 polyamide materials. The aim of this study is to determine the surface properties of natural and glass reinforced PA66 plates, to compare the 2D surface roughness parameters (Ra, Rz, Rq, Ry) of the two selected engineering polymers and to evaluate the effect of cutting speed and feed rate on the surface parameters. This information will provide insight into how to improve milling technology to optimize the surface quality required for different industrial applications.

Contributing department: Technical Institute

Outsider consultant:

Insider consultant: Dr. Gábor KALÁCSKA university instructor, MATE, Technical Institute

Deadline of thesis submission: 2024 year 04 month 22 day

Date: Gödöllő, 2024 year 04 month 17 day



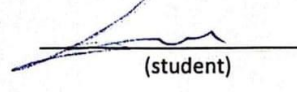
(head of department)

I approve



(specialist coordinator)

Received



(student)